ANALYSIS OF SOLAR POWER AS SINGLE SOURCE OF ELECTRICITY FOR MIDDLE EAST AND NORTH AFRICA COUNTRIES

by
Manuel Jose Millan Sanchez

A capstone submitted to Johns Hopkins University in conformity with the requirements for the degree of Master of Science in Energy Policy and Climate Change

Baltimore, Maryland
April 2018

Abstract

The power sector is living a revolution. The cost of clean technologies is declining faster than expected and deployment targets are being achieved with relative easiness. However, as of today, to think of an entire renewable power sector still seems a utopic objective because of two main factors: variability of renewable resources and cost competitiveness with conventional sources. A lot has been written about the future of solar technologies. Different paces of cost decline of solar photovoltaics (PV) and concentrating solar power (CSP) in the recent times creates uncertainty about the predominance of one or the other. Additionally, while PV is much cheaper nowadays, CSP can provide dispatchable electricity which is highly valued in order to instantaneously balance demand and supply. Battery systems (BESS) to be integrated with PV may seem offer a feasible alternative, but the costs of batteries are still high. Different entities are trying to forecast the cost evolution for these technologies but there is still no consensus about a long-term predominance of any of these technologies for providing 24-hour solar-based generation.

The present study intends to analyze the possibility of supplying an entire national system with solar energy only, comparing the different possible alternatives face to face. The analysis uses the two mentioned solar technologies: PV and CSP for providing electricity 24/7 in fifteen different countries. The selected geographic area for the study is the MENA region, which counts with excellent solar resources and developed power systems. The study simulates an economic dispatching of solar generation technologies, optimizing the total cost of generation for one year in different cost scenarios (2017, 2025 and 2030) using the existing future cost projections for both technologies.

This analysis assumes that the only available technologies for supply the whole demand in the countries are these two solar technologies, ignoring hypothetically, the actual existence of other technologies. It intends to shed some light about how two solar technologies—namely solar

photovoltaics with battery systems and concentrated solar power—can coexist in a power system and how we can compare the techno-economic performance of both on a level playing field

The analysis is based on a linear programming model that minimizes the annual cost of electricity generation following the load profile and radiation in each country. A common base of 100 MW peak demand has been adopted for the sake of simplicity and comparability.

The main findings of the study show that:

- Solar technologies only (with storage) can be a feasible alternative for providing power to an entire system. However, solar technologies are still far from being a competitive option when compared with conventional sources, although, if costs evolution is as expected, it might be in line with them by 2030. Moreover, in countries where baseload is based on oil fired plants solar baseload might be already competitive.
- Assuming the expected forecasts for the technologies cost evolution, cost is not the only and/or main driver. The availability of their respective solar resource (DNI and GHI) will still be a critical factor for optimizing the generation mix. This critical role of solar resource will be accentuated as technologies costs decrease.
- Finally, solar technologies are complementary in almost all scenarios. Whatever is the cost evolution both technologies are always present and none of them is completely discarded. In terms of storage technologies, the study shows that thermal storage associated with CSP is heavily predominant over BESS.

Table of Contents

Table of figures

List of Tables

Abbreviations and Acronyms

AC	Alternating current
BESS	Battery Energy Storage System
CSP	Concentrating Solar Power
CRS	Central receiver system
DC	Direct current
DE	Parabolic dish Stirling
DHI	Diffuse Horizontal Irradiation
ECMWF	European Centre for Medium-Range Weather Forecasts
EU	European Union
GHI	Global Horizontal Irradiation
KSA	Kingdom of Saudi Arabia
LCOE	Levelized Cost of Electricity
LF	Linear Fresnel
MENA	Middle East and North Africa
NOAA	National Oceanic and Atmospheric Administration
PV	Photovoltaics
PT	Parabolic trough
SoC	State of charge
TES	Thermal Energy Storage
UAE	United Arab Emirates

1. Introduction

The electric system is experimenting a revolution in the last decades. With growing interest in renewable energy, the penetration of these resources is rising at a very high rate (J. Jorgenson, P. Denholm, and M. Mehos 2014). Continuous years of policy support combined with rapid technology development from public and private entities has made renewable energy a real and competitive option to produce electricity at massive and affordable levels. This fact is creating a virtuous circle of investment-innovation-cost reductions that is retrofitting the change in the electricity industry. In 2015, 23.6% of the total world electricity was produced from renewable sources (Figure 1-1). Renewable power generation capacity grew by 154 GW, an increase of 9.3% over 2014. Most of the new capacity came from wind (66 GW) and solar PV (47 GW) (IRENA 2017). Both technologies have exceeded the capacity of hydropower for the first time.

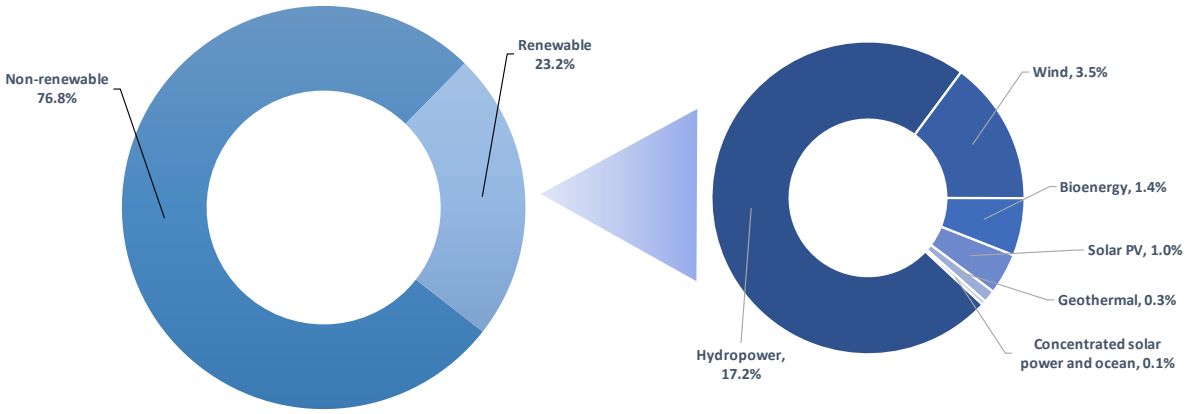

Figure 1-1 Global electricity generation by source, 2015 (IRENA 2017))

Moreover, the electricity sector has become the main focus of the Paris Agreement[1]. In the main scenario to accomplish the target of the agreement, nearly 60% of all new power generation capacity to 2040 in our main scenario comes from renewables. Thus, by 2040, solar PV is expected to see its average cost cut by a further 40-70% and onshore wind by an additional 10-25% (IEA 2016). This scenario depicts a promising future, where a power system purely supplied by renewable energies can be envisaged.

However, from a system perspective, this scenario has some technical challenges to be solved. Accommodating the uncertainty of some variable sources (namely solar PV and wind) will be a challenging aspect of integrating large-scale renewable energy into the electric power system. Currently, concentrating solar power (CSP) with thermal energy storage (TES) is the sole affordable source of solar energy whose output can be shifted over time and also controlled in response to system operator signals, allowing for provision of a wide range of grid services (J. Jorgenson, P. Denholm, and M. Mehos 2014). For other time-varying sources, cutting-edge technologies are rising as Battery Electricity Storage Systems (BESS) that could help to balance demand and variable supply. However, these technologies, although very promising, are still not competitive with other dispatchable sources.

The comparison of both solar technologies is however complicated. Their disparity of features (nominal power and storage capacity), system-level characteristics (demand variability), and geographical specificity (solar radiation) make very difficult to compare both technologies for setting general rules. This lack of generalizable rules poses a heavy burden when power system planners are considering these options. As they cannot rely on general numbers, they need to

[1] The Paris Agreement is an agreement within the United Nations Framework Convention on Climate Change (UNFCCC) dealing with greenhouse gas emissions mitigation, adaptation, and finance starting in the year 2020. The language of the agreement was negotiated by representatives of 196 parties at the 21st Conference of the Parties of the UNFCCC in Paris and adopted by consensus on 12 December 2015.

perform location-specific studies to determine which of them are more suitable for the medium and long-term. Moreover, the rapid evolving environment of these technologies, regarding features and costs, is an additional burden when medium and long-term planning exercises are being made.

The present study intends to shed some light about how solar technologies can coexist in a power system and how we can compare both on a level playing field. For that exercise, the study presents scenarios of individual national systems that are intended to be fully supplied by renewable solar systems (PV and CSP). The study has been carried out for fifteen countries of the Middle East and North African region (MENA), rich in solar resource. The study has been limited to solar energy because it is reasonably homogeneous in these countries and way more abundant than wind resources. The analytical framework for the study has been depicted in Figure 1-2.

Finally, the objective of the study can be defined by trying to respond to two key questions related to the future of renewable solar energy and its role in future power systems:

- Can solar technologies be the only power generation source for entire national and/or regional power systems at a competitive cost?
- Considering the expected improvements in technologies and prices of the different solar technologies and storage systems, what technology can be expected to have the most promising future to entirely supply the whole demand of a power system at a competitive cost? In other words, what are the drivers that define the adequacy of a solar technology in a specific geographical location?

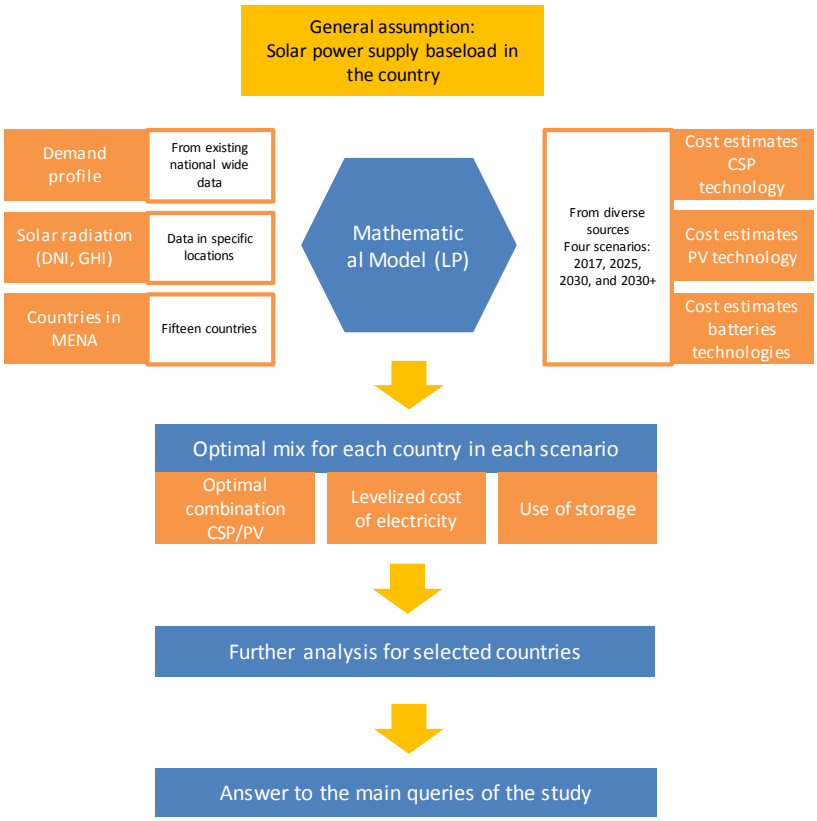

Figure 1-2 Analytical framework

2. Technologies description

2.1. Solar power

Availability of solar resource is the most determining element in the evaluation of the performance of solar plants. It is a function of geographical and meteorological aspects, and it is expected to vary both at the regional level and at the individual country level. Furthermore, local features at a given site, such as orography, altitude, inclination, vegetation etc. have also influence on the solar resource that can be attained.

2.1.1. Solar irradiance and irradiation

In order to analyze the solar resource, we should distinguish first the following two concepts:

- Irradiance is the amount of electromagnetic energy incident on a surface per unit time per unit area, or radiant power per unit area (flux). It can be expressed in kW/m² (or W/m²).
- Insolation or Irradiation is the radiant energy received per unit area (over a given period of time), or irradiation summed over time. It can be expressed in kWh/m²day (or kWh/m²year).

The solar irradiance at a given moment on a solar collector placed on the Earth surface depends on several factors (Kalogirou 2013):

- The solar radiation reaching earth (extraterrestrial radiation, i.e. incident at the top of the earth's atmosphere).
- The position of the Sun in the sky at that given moment (generally defined by the azimuth and elevation angles) and the altitude of the site, which represent the length of the trajectory of solar radiation through the atmosphere to reach the ground.
- The atmospheric conditions which will influence the amount of the radiation that will reach the ground, directly or after being scattered.
- The orientation of the collector relative to the direction of the sun rays.
- The presence of obstacles between the collector and the sun rays, blocking part of the solar radiation that would otherwise be caught by the collector (shadow).

2.1.2. Extraterrestrial solar radiation

The average irradiance on a surface perpendicular to incoming radiation above the atmosphere (at the mean distance of the Earth from the Sun) is called the solar constant. The accepted solar constant is 1,368 W/m^2 (Kalogirou 2013).

The actual extraterrestrial irradiance on a surface perpendicular to incoming radiation at the top of the atmosphere for a given latitude varies throughout the day with the Earth's rotation and throughout the year with the Earth's declination δ.

The Earth's axis is tilted approximately 23.45 degrees concerning the earth's orbit around the sun (Figure 2-1). This value is constant during the year. Due to the Earth's axis, the Sun is higher in the sky during summer and lower in the sky when winter approaches. The Earth's declination is the angle between the earth's axis and a plane perpendicular to an imaginary line drawn between the Earth and the Sun (Solar Radiation Monitoring Laboratory. University of Oregon 2002). It is variable during the year (between + and -23.5°), and leads to different lengths of days and nights during the year.

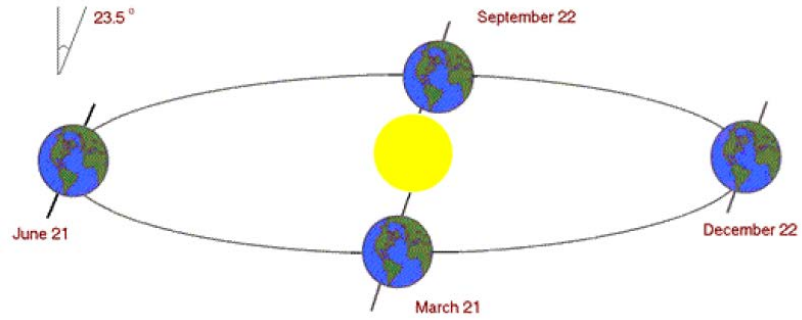

Figure 2-1 Earth orbit around the Sun and declination angle

2.1.3. Terrestrial solar radiation

The terrestrial solar radiation, which is the one to be considered for terrestrial applications like CSP and PV plants, differs from the extraterrestrial solar radiation due to the atmospheric effects.

From the origin in the sun, solar rays follow a trajectory parallel to the direction sun-earth. As the sunlight passes through the atmosphere, a large portion of the UV radiation is absorbed and scattered by air molecules and suspended particles (water vapor and dust) (Solar Radiation Monitoring Laboratory. University of Oregon 2002). The scattering results in the deviation of part of the sun rays in all directions. Part of the scattered rays will reach the ground, and part of it will

be scattered back into space. The scattered radiation reaching the Earth's surface is called diffuse radiation (Figure 2-2).

The scattering and absorption by air molecules is not the same for all wavelengths (Kalogirou 2013). As a consequence, the spectrum of terrestrial solar radiation differs from that of the extraterrestrial solar radiation.

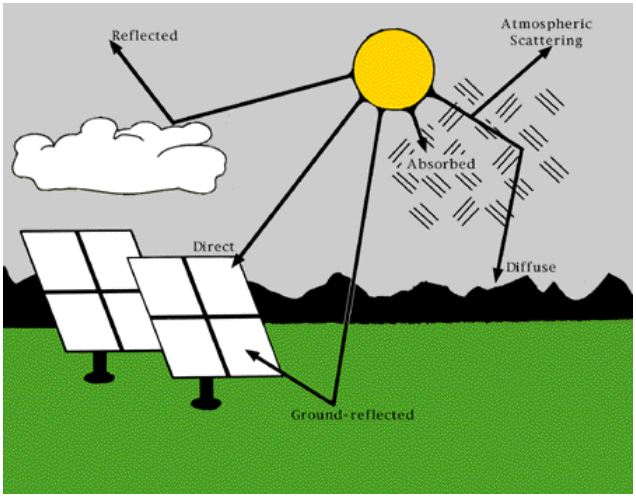

Figure 2-2 Atmospheric effects. Source: NREL website

Some radiation is also reflected by the ground and then re-scattered by the atmosphere to the observer: it is the albedo radiation. For some ground coverage (snow, etc.) this can represent a significant part of the radiation perceived by an observer (Kalogirou 2013).

Depending on the relative position of the sun in the sky, the air mass the sun rays must cross before reaching the ground will vary. Therefore, the proportion of the extraterrestrial irradiance that reaches ground level will be reduced when the sun is lower in the sky. Note that locations at a higher altitude (mountainous areas), experience a reduced air mass; in that case, the solar radiation undergoes less diffusion and absorption before reaching the ground.

Global Horizontal Radiation also called Global Horizontal Irradiance is the total solar radiation; the sum of Direct Normal Irradiance (DNI), Diffuse Horizontal Irradiance (DHI), and ground-reflected radiation, which is usually insignificant:

$$GHI = DHI + DNI\cos\theta \quad (\theta\ is\ the\ solar\ zenit\ angle)(\frac{W}{m^2})$$

While photovoltaic effect uses energy from the GHI, the concentrated solar effect only uses the one from DNI. This fact is significant when analyzing the different performance of plants in different locations.

2.2. Concentrating solar power (CSP)

Solar energy has a high exergetic value since it originates from processes occurring at the sun's surface at a blackbody equivalent temperature of approximately 5777 K. Due to this high exergetic value, more than 93% of the energy may be theoretically converted to mechanical work by thermodynamic cycles (Manuel Romero-Alvarez, Eduardo Zarza 2007). The conversion of solar heat to mechanical work is limited by the Carnot efficiency, and therefore to achieve maximum conversion rates, the energy should be transferred to a thermal fluid or reactants at temperatures close to that of the sun.

Even though solar radiation is a source of high temperature and energy at origin, with a high irradiance of 63 MW/m^2 (Kalogirou 2013), the irradiance available for terrestrial use only slightly higher than 1 kW/m^2. It is, therefore, an essential requisite for solar thermal power plants to make use of optical concentration devices that enable the thermal conversion to be carried out at high solar flux and with relatively little heat loss. A simplified model of a concentrating solar thermal power (CSP) plant is depicted in Figure 2-3 (Manuel Silva 2005).

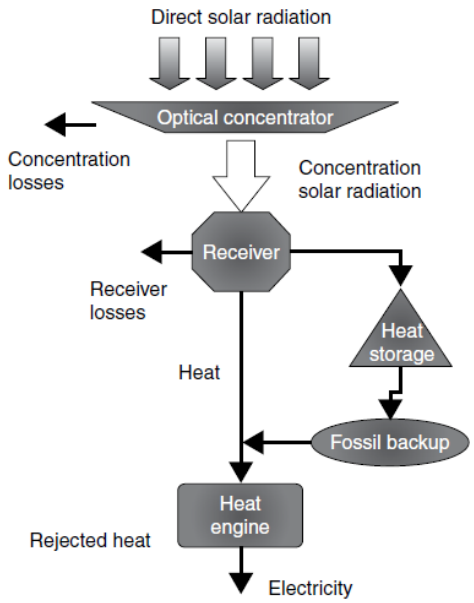

Figure 2-3 Flow diagram for a typical solar thermal power plant (Manuel Romero-Alvarez, Eduardo Zarza 2007)

The excellent CSP system design combines a relatively large, efficient optical surface (e.g., a field of high-reflectivity mirrors), harvesting the incoming solar radiation and concentrating it onto a solar receiver with a small aperture area. The solar receiver is a high-absorption and transmittance, low-reflectance, radiative/convective heat exchanger that emulates as closely as possible the performance of a radiative black body. An ideal solar receiver would have negligible convection and conduction losses (Manuel Romero-Alvarez, Eduardo Zarza 2007).

In the case of a solar thermal power plant, the solar energy is transferred to a thermal fluid at an outlet temperature high enough to feed a heat engine or a turbine that produces electricity. The solar thermal element can be a parabolic trough field, a linear Fresnel reflector field, a central receiver system or a field of parabolic dishes (Figure 2-5), commonly designed for a normal incident radiation of 800–1000 W/m^2. Annual DNI varies from 1,600 to 2,800 kWh/m^2 depending on the available radiation at the particular site.

Solar transients and fluctuation in irradiance can be mitigated by using an oversized mirror field (solar multiple[2] higher than 1) and then making use of the excess energy to load a thermal or chemical storage system. Hybrid plants with fossil backup burners connected in series or in parallel are also possible. The use of heat storage systems and fossil backup makes CSP systems highly flexible for integration with conventional power plant design and operation and for blending the thermal output with fossil fuel, biomass and geothermal resources. Also, hybridization is possible in power booster and fuel saver modes with natural gas combined cycles and coal-fired Rankine plants and may accelerate near-term deployment of projects due to improved economics and reduced overall project risk. As a consequence, CSP can currently supply transferable power and meet peaking and intermediate loads at the lowest electricity costs of any grid-connected solar technology (Manuel Romero-Alvarez, Eduardo Zarza 2007).

Regarding electricity grid and quality of bulk power supply, CSP can provide dispatchability[3] on demand that makes CSP stand out from other renewable energy technologies like PV or wind. Even though the sun is an intermittent source of energy, CSP systems offer the advantage of being able to run the plant continuously at a predefined load. Thermal energy storage systems store excess thermal heat collected by the solar field. A typical storage concept consists of two storage tanks filled with a liquid storage medium at different temperatures. When charging the storage, the medium is pumped from the “cold” to the “hot” tank being heated up (directly or indirectly) by the solar heat collected. When discharging, the storage medium is pumped from the “hot” to the “cold” tank extracting the heat in a steam generator that drives the power cycle. Storage systems, alone or in combination with some fossil fuel backup, keep the plant running under full-load conditions.

[2] Solar multiple is defined as the ratio between the thermal power produced by the solar field at the design point and the thermal power required by the power block at nominal conditions. (M.J. Montes 2009)
[3] Dispatchability refers to the ability of electricity generation sources to be dispatched at the request of power grid operators or of the plant owner according to market needs.

Storing thermal energy allows the managers of the plant to know when the plant must stop supplying energy. Figure 2-4 shows how stable operation can be extended for several hours after sunset (Manuel Romero-Alvarez, Eduardo Zarza 2007).

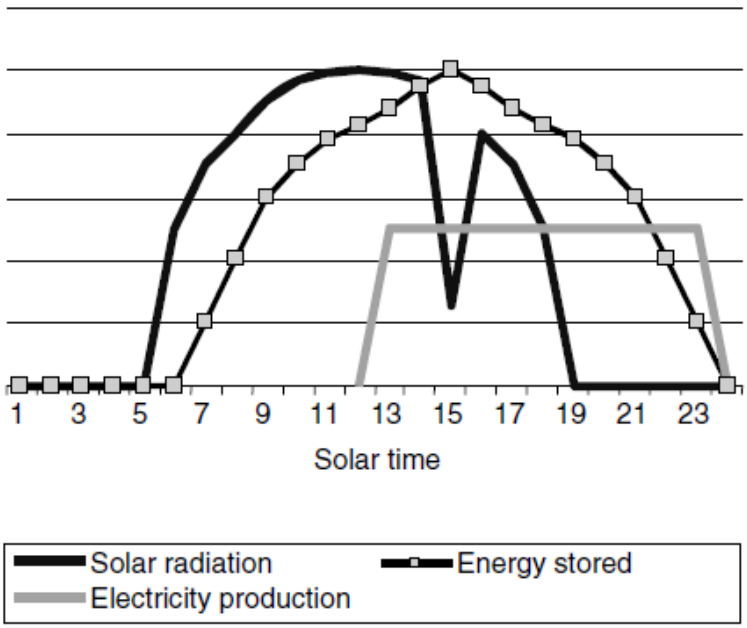

Figure 2-4 Extended operation with solar-only CSP plant with some hours of TES (Manuel Romero-Alvarez, Eduardo Zarza 2007)

This capability of storing high-temperature thermal energy leads to economically competitive design options, since only the solar field and the thermal storage need to be oversized. This fact means that there is an incremental cost for the storage system and additional solar field, while the size of the conventional part of the plant (power block) remains the same.

Four concentrating solar power technologies are today represented at pilot and demonstration-scale: parabolic trough collectors (PT), linear Fresnel reflector reflectors (LF), power towers or central receiver systems (CRS), and parabolic dish/engine systems (DE) (Manuel Silva 2005).

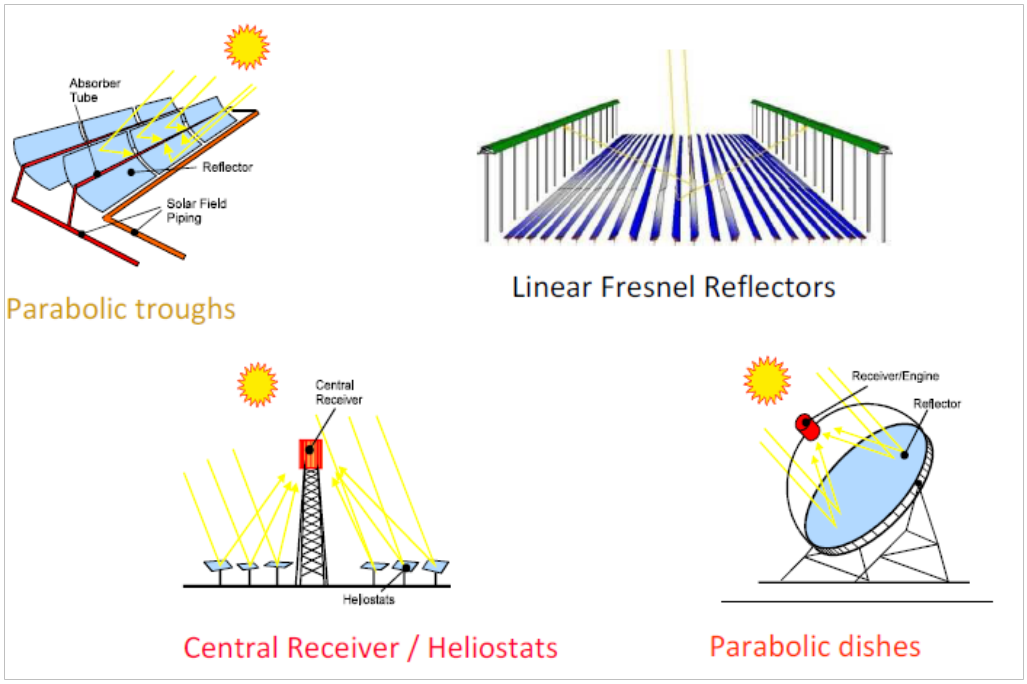

Figure 2-5 Schematic diagrams of the four CSP systems scaled up to pilot and demonstration sizes.

PT and LF are 2D concentrating systems in which the incoming solar radiation is concentrated onto a focal line by one-axis tracking mirrors. They are able to concentrate the solar radiation flux 30–80 times, heating the thermal fluid up to 393°C, with power conversion unit sizes of 30–150 MW, coupled with a Rankine steam turbine/generator cycle.

CRS optics are more complex, since the solar receiver is mounted on top of a tower and sunlight is concentrated by means of a large paraboloid that is discretized into a field of heliostats. This 3D concentrator is therefore off-axis and heliostats require two-axis tracking. Concentration factors are between 200 and 1000 and unit sizes are between 10 and 200 MW. Therefore, they are well suited for dispatchable markets and integration into advanced thermodynamic cycles. A wide variety of thermal fluids, like saturated steam, superheated steam, molten salts, atmospheric air or pressurized air, can be used, and temperatures vary between 300 °C and 1000 °C.

Finally, DE systems are small modular units with autonomous generation of electricity by Stirling engines or Brayton mini-turbines located at the focal point. Dishes are parabolic 3D concentrators

with high concentration ratios (1000–4000) and unit sizes of 5–25 kW. Their current market niche is in both distributed on-grid and remote/off-grid power applications.

Table 2-1 (IRENA 2012) show typical solar-to-electric conversion efficiencies and annual capacity factors, for the four technologies.

	PT	LF	CRS	DE
Operating temperature (°C)	350-550	390	250-565	550-750
Annual Capacity factor	25-28% (no TES) 29-43% (7h TES)	22-24%	55% (10h TES)	25-28%
Peak efficiency	14-20%	18%	23%	30%
Annual Solar-to-electricity efficiency	11-16%	13%	7-20%	12-25%

Table 2-1 Efficiency parameters for the main CSP technologies

This study focuses on the current most promising technology in terms of capacity factor and efficiency: the central receiver system or power tower with thermal storage in molten salts.

2.2.1. Central receiver system with thermal storage in molten salts

In power tower plants, also known as central receiver systems, a field of hundreds or thousands of heliostats (large two-axis tracking individual mirrors) is used to concentrate sunlight 600 to 1000 times onto a central receiver mounted at the top of a tower (Breeze 2014). The field of heliostats, which all move independently of one another, can either surround the tower (surround field) for larger systems or be spread out on the shadow side of the tower (North field in the Northern hemisphere) in the case of smaller systems (Figure 2-6).

Due to the high concentration ratios, high temperatures can be reached, resulting in increased efficiency of heat to electricity conversion and reduced cost of thermal storage. Within the receiver, a heat transfer fluid absorbs the highly-concentrated radiation reflected by the heliostats and converts it into thermal energy to be used in a conventional power cycle. The power tower concept

can be incorporated with either a Rankine steam turbine cycle or a Brayton gas turbine cycle, depending on the applied heat transfer fluid and the receiver concept. Some plants have modular designs, with several towers that feed one power block.

In a molten salt power tower plant, the cold salt (290°C) is pumped from the cold tank to the receiver, where the salt is heated up to 565°C by the concentrated sunlight. The hot salt is then pumped through a steam generator to generate superheated steam that powers a conventional Rankine cycle steam turbine. The solar field is generally sized to collect more power than demanded and by the steam generation system and the excess energy can be accumulated in the hot storage tank.

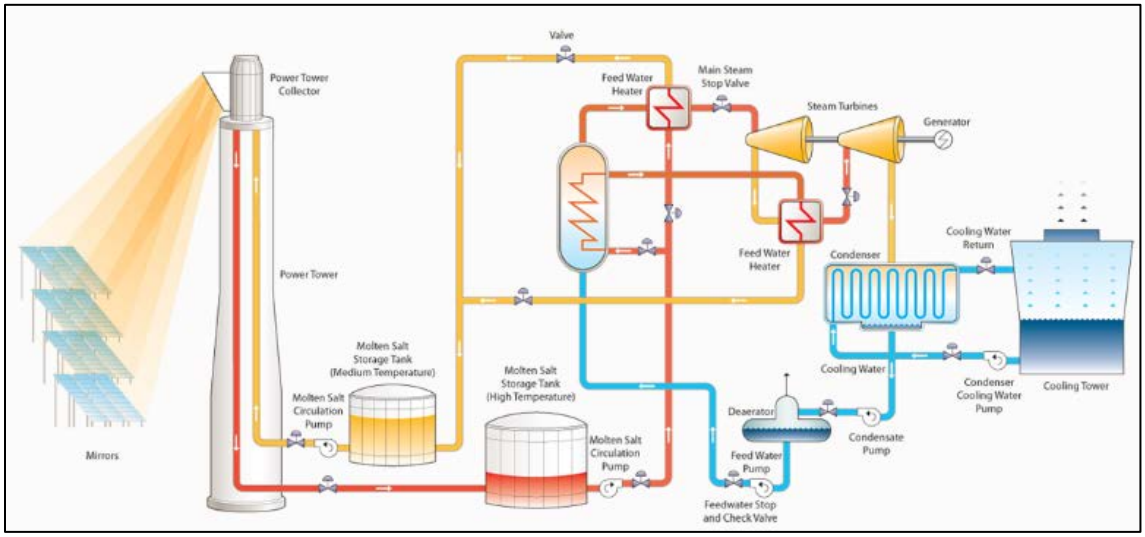

Figure 2-6 Schematic of molten salt power tower with steam turbine cycle

2.2.2. Thermal storage for central receiver systems

In central receiver systems using molten salts as heat transfer fluid, the thermal storage is an inherent part of the system. The salts from the cold tank are heated in the receiver and directly stored in a hot salt tank. The steam generator oppositely uses the circuit taking salts from the hot tanks and returning them to the cold tank. Thus, the steam generation is completely delinked of the solar radiation. Making tanks bigger, and consequently the solar generation device, the system will have the capability to generate electricity for more time, even after daylight period.

There are significant advantages brought by the implementation of Thermal Energy Storage (TES), the most striking one being the possibility of making CSP dispatchable. Dispatchability offers power generation that is less reliant on weather conditions, allowing plants to increase their flexibility and operational range resembling traditional while decreasing the levelized cost of electricity generated by a CSP plant.

Furthermore, it also enables the plant to provide ancillary services. The most important benefits of TES with CSP include the following:

- Capacity factor: The capacity factor can be increased from 20-25% of plants without storage to values up to 60-70%, associated with an integrated storage capacity of 13-14 hours. Such features make CSP a suitable technology for the base load operation.
- Shifting generation: Besides base load operation, flexibility brought by storage makes possible to consider shifting from periods of low demand, when the energy price is lower, to peak demand periods associated with high costs of electricity, thus maximizing the economic performance of the plant.
- Avoidance of intermittency: Thermal storage can compensate for the fluctuating behavior of the solar resource, thus reducing transient operation in power generating units and improving stability/performance.
- Frequency response: Frequency response is an ancillary service provided by conventional generators consisting of varying their power output ato maintain the frequency of the grid. Integration of storage allows CSP to be able to provide frequency response services, making the technology more competitive with conventional generation.
- Lower LCOE: Although the adoption of TES in CSP plants leads to increased capital needs, it also implies a reduction in the levelized cost of electricity due to the higher capacity factor that compensate the higher investment costs.

2.3. Solar photovoltaics (PV)

Solar PV absorbs direct normal irradiance (DNI), diffuse horizontal irradiance (DHI) and reflected components, all of which sum up making global horizontal irradiance (GHI). PV cells directly convert this solar energy into electricity through the photovoltaic effect. When photovoltaic material receives a photon, it can be absorbed, reflected or transmitted. In the case where it is absorbed, and if the energy of photon is greater than the band gap of the semiconductor, an electron can be released and removed through the help of the p-n junction of the material. The electron is free to flow as a current through the creation of an electric field between the n-type and p-type semiconductors. There are two many types of PV cells available today: (i) Crystalline silicon (c-Si); and (ii) Thin film (TF) (Quaschning 2004). Crystalline silicon cells currently dominate the market with a share of approximately 90%, while thin film is represented by approximately a 10% share.

The performance of a PV cell, module or array can be visualized with an I-V curve, which describes the maximum power point for given weather conditions, i.e. the PV panel's rated power under a specified condition, usually standard testing conditions (STC). STC means that the solar panels are tested with irradiation of 1000 W/m^2 under cell temperature conditions of 25 °C and assuming an air-mass of 1.5. Air-mass is the optical path length through the Earth's atmosphere for light where the air-mass at the equator is 1. Two main parameters significantly affect the performance of a PV panel: (i) solar irradiation; and (ii) ambient temperature. It is very important that these two parameters are taken into consideration when designing a PV array.

A PV plant consists of several PV strings connected in parallel to a centralized inverter. The inverter is necessary because the power output is direct current (DC) and must be converted to alternating current (AC). Each PV string consists of a number of PV modules connected in series each with a

bypass diode. The bypass diode is included to protect the system from irregular irradiation or partial shading. Connecting PV modules in series increases the voltage of the system and connecting the PV strings in parallel increases the current of the system.

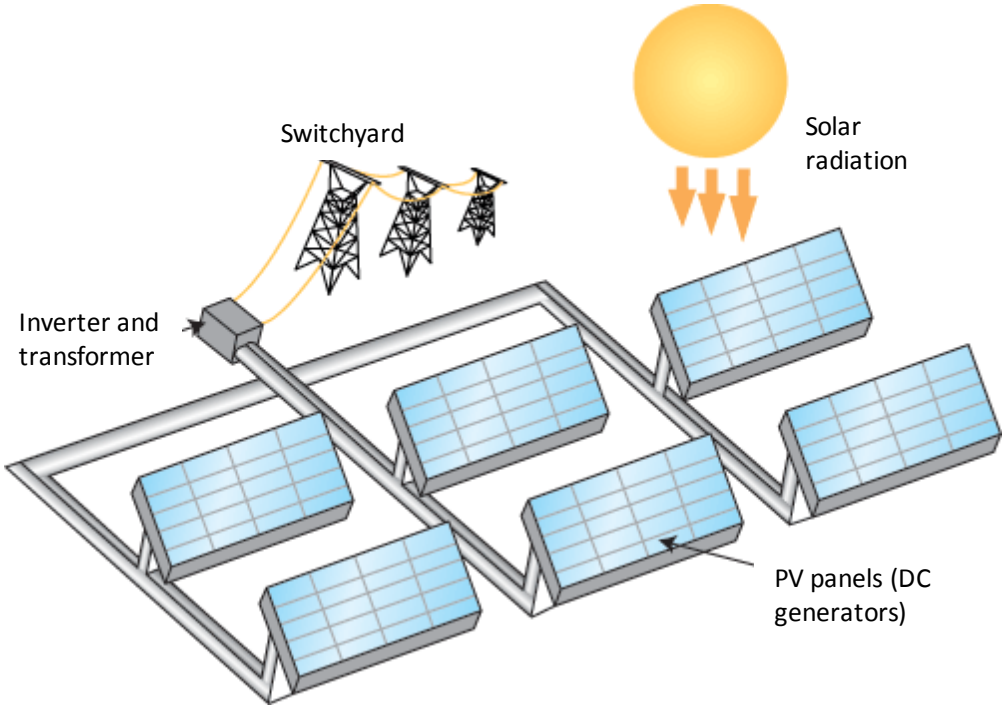

Figure 2-7 Simplified PV plant configuration

The PV plant can also include a battery energy storage systems (BESS) to compensate the fluctuations of the solar resource and extend the operating hours of the system, resulting in improved capacity factor and flexibility.

2.4. Battery Energy Storage Systems (BESS)

Due to high capital and maintenance cost and current technical limitations, such as lifetime, capacity, self-discharge rates etc., battery energy storage systems (BESS) have not been used yet at large scale in utility-scale applications. The successful implementation of BESS at large scale combined with PV might represent a potential breakthrough for the future large-scale diffusion of solar electricity generation. However, so far, large scale application of these batteries can be found today only for ancillary grid services of frequency control and spinning reserve.

The main types of batteries available today are the following: lead-acid, nickel cadmium, nickel metal hydride, lithium ion, sodium sulfur and flow batteries. Lead-acid may represent the most mature technology and is currently being used in PV applications. Nickel cadmium is a mature technology at the appliance level, but its use for high capacity applications is also being explored. Compared to lead acid, nickel cadmium offers longer life cycles, higher energy densities and lower maintenance requirements but its main drawbacks include the use of toxic heavy metals, its large dimensions and high self-discharge rates. A utility-scale application of this technology is represented by the battery park deployed in Alaska, which is able to provide 27 MW for 15 min or 46 MW for 5 min for grid support services such as spinning reserve, frequency regulation, VAR support etc. Nickel metal hydride can be seen as an advancement of the nickel cadmium by being more environmentally friendly and presenting 25-30 percent higher energy densities. Its main drawbacks are high self-discharge rates and scarce availability of the battery materials. Sodium sulfur batteries are high temperature devices which operate in the 300-350 °C range. They are mainly employed for stationary applications. The largest system up to date is the newly built 350 MWe battery park in the United Arab Emirates by the Amplex Group, used for grid stabilization and support purposes. Flow batteries are a modern concept currently under study. Unlike conventional batteries, flow batteries use electrolyte solutions stored in external tanks, making these batteries highly scalable according to the chosen dimensions of the tanks. They feature high efficiency, short response times, symmetrical charge and discharge and quick cycle inversion. On the other hand, low energy densities, the toxicity of the materials and early stage of development make these batteries more likely to play a role in small-scale applications in the near future.

Lithium-ion batteries are the most promising technology for large-scale storage applications. Although usually confined to the portable electronics market, their characteristic makes them extremely attractive for renewable energy application in the medium term. In fact, their storage

efficiency reaches almost 100% and they feature the highest energy density amongst all. The implementation at very large scale is already a commercial reality with plenty of facilities around the globe. Recently, a 100 MW-4 hours lithium ion facility has been announced to be developed in California to provide peak load support for replacement of gas fired power plants.

3. Geographical context of the study

3.1. Power sector in Middle Eastern countries

The study will concentrate on the MENA region, with a focus on the fifteen countries indicated in Figure 3-1.

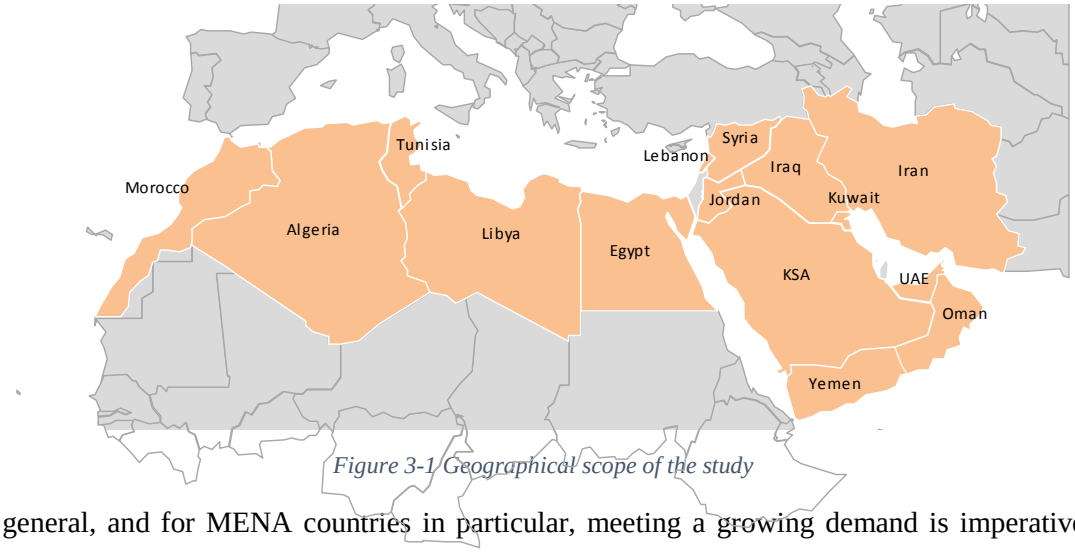

Figure 3-1 Geographical scope of the study

In general, and for MENA countries in particular, meeting a growing demand is imperative to ensuring continued economic growth. Given the undergoing population growth and economic expansion in the region, there is an increasing need to invest in electric power generation capacities and in the transmission and distribution networks of countries in the MENA region (The Economist 2011).

The region presents two types of countries, facing different issues regarding how to undertake the rise on power demand. For oil-importing nations, access to funding is an obstacle to ensure adequate supplies of power for the future, while for oil-exporting states, the covering of power

demand is consuming their national main source of revenues. The result of these opposite problems is a downwards spiral resulting in countries in the MENA region experiencing power shortages.

Although, until now, MENA countries have relied on fossil fuels (natural gas and oil) to generate electricity, MENA countries are recently diversifying fuel sources and investing in renewables, especially solar power. As part of the efforts to expand power supply, some MENA countries are diversifying their fuel mix in order to secure continued access to primary energies. According to the IEA, around 7% of the region's power will come from renewable sources by 2030, up from just 3% today.

Brand-new nuclear power and regional grid will have a significant impact. Nuclear power, expected to become available in the UAE in the coming years together with the GCC regional grid, is likely to have a very significant impact on power supply in the MENA region (The Economist 2011)

Energy efficiency initiatives are emerging in the region. Policymakers in some countries are promoting efficiency among power consumers, for example through mandatory building regulations in Abu Dhabi, and through variable time-of-day power tariffs in Saudi Arabia (The Economist 2011).

Low electricity prices, mostly due to national subsidies, are the main obstacle to implement demand management programs. Some MENA countries continue to subsidize electric power, giving little incentive for consumers to economize and to shift consumption patterns. Governments appear to be reluctant to reduce these subsidies, yet subsidy reductions are critical if power demand is to be managed (The Economist 2011).

4. Methodology and modeling

4.1. Study method

The study has been developed following a supply-demand configuration. While most modeling efforts of solar plants are based on supplying a limited demand—normally during daylight and some hours after for CSP plants—, this study proposes that solar technologies follow the demand curve in the countries analyzed. The traditional analysis of solar plants omits the possibility of having solar operating as a baseload technology, or as a sole electricity production source. The perspective of this study is to inform about the feasibility of solar to supply an entire power system as the sole generation technology.

The model developed for this study calculates the optimal capacity mix of solar technologies under different cost scenarios in order to cover the whole electricity needs for individual country power systems. The model is based on a linear programming formulation that minimizes generation costs and determines the least-cost mix for a number of different technology cost scenarios. Such minimization is subject to a set of system-level constraints (e.g., demand balance equations) and technology-specific constraints (e.g., resource availability constraints). The complete model formulation is included in Appendix 1.

In order to define the cost scenarios, each technology has been preliminarily decomposed in its correspondent cost structure. These cost structures combine the elements in each technology elements that are functionally linked and whose design parameters and costs are proportional to the same plant attribute (i.e., energy that can be stored, power that can be delivered, etc.), making them likely to evolve at the same pace. In particular, each technology considered (CSP, PV) has been structured in the following components:

- Concentrated Solar Power
    - Component CSP-A. Solar field. Defined per m^2 of capture (mirrors). It includes all the heliostats field and its respective auxiliary equipment.
    - Component CSP-B. Receiver. Defined per MWth of capacity. It includes auxiliary equipment.
    - Component CSP-C. Thermal storage. Defined per MWhth. It includes all equipment associated with the thermal storage such as tanks, molten salts, salts-water exchanger and their respective auxiliary equipment.
    - Component CSP-D. Power block. Defined per MW electric gross. It includes all equipment associated with the steam cycle and its respective auxiliary equipment.
- Solar Photovoltaics (PV):
    - Component PV-A. Solar field. Defined per m^2 of PV panels. It includes all panels with electrical connections up to the inverters.
    - Component PV-B. Balance of Plant. Defined per MW electric gross. It includes all equipment associated with electricity delivery to the grid, inverters (included in this component), transformers and all auxiliary equipment.
    - Component PV-C. Battery Energy Storage System (BESS). Defined per MWh electric. It includes the batteries themselves and all auxiliary equipment.

The study is carried out in four temporal scenarios: current scenario or high cost (2017), medium cost scenario (2025), and low-cost scenario (2030). Each of these scenarios are points in time when the technologies are assumed to have evolved and each component has a cost forecast. Each technology is separately built upon these components and its cost is calculated following the cost defined for each of its components in each scenario. Section 5.3 includes the cost estimation for each of the component in each scenario.

4.2. Functional model

The operational diagram for the two solar technologies studied is presented in Figure 4-1. As depicted, each technology is built upon its respective components. The components are functionally linked by the technology internal equations. These equations are built upon the different variables, which are defined later in this section. The model analyzes hourly generation for one year (8,760 hours) and calculates the optimal size of each component and therefore, the optimal mix of both technologies in the grid to optimally follow the demand.

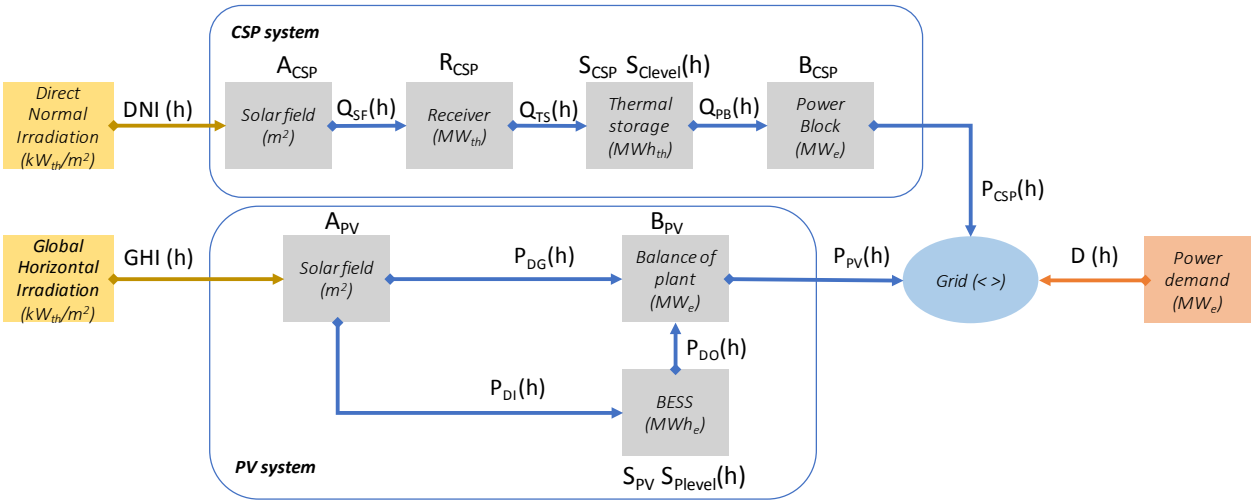

Figure 4-1 Functional block model

This model is run hourly for one full year and optimizes the costs of the system over that period, including annual investment amortization and annual Operation and Maintenance costs.

4.3. Mathematical model

The operational diagram in Figure 4-1 and the relationships between the different elements of the two technologies considered have been modeled through a set of mathematical equations, representing behaviors inherent to the technologies and to the system. Modeling the physical processes taking place in each of the blocks represented involve making several assumptions in

terms of internal efficiencies and functional parameters. Those have been drawn from selected bibliography and information from manufacturers of equipment. The values and sources for the main parameters used are indicated in table ..... INDICATE WHERE

The model has been divided into two blocks: the constraint relations and the objective function. These two blocks are described below.

4.3.1. Constraints

Constraints Concentrated Solar Power system

Constraint (1). Solar field generation

$$Q_{SF}(h) \leq DNI(h) * A_{CSP} * \rho_{SF}(h) * \rho_{REC}$$

Heat collected by the CSP solar field at every hour $Q_{SF}(h)$ is lower or equal to the normal radiation (DNI(h)) incident in the total receiver area (A_{CSP}). Different performances are to be applied.

$\rho_{SF}(h)$ is the performance of the solar field. This value is defined in terms of the optical efficiency, which is equal to the ratio of the net power intercepted by the receiver to the product of the direct insolation times the total mirror area. The optical efficiency includes the cosine effect, shadowing, blocking, mirror reflectivity, atmospheric transmission, and receiver spillage. Several optical loss factors are illustrated in Figure 4-2 and explained below since they determine the solar field modeling (Falcone 1986).

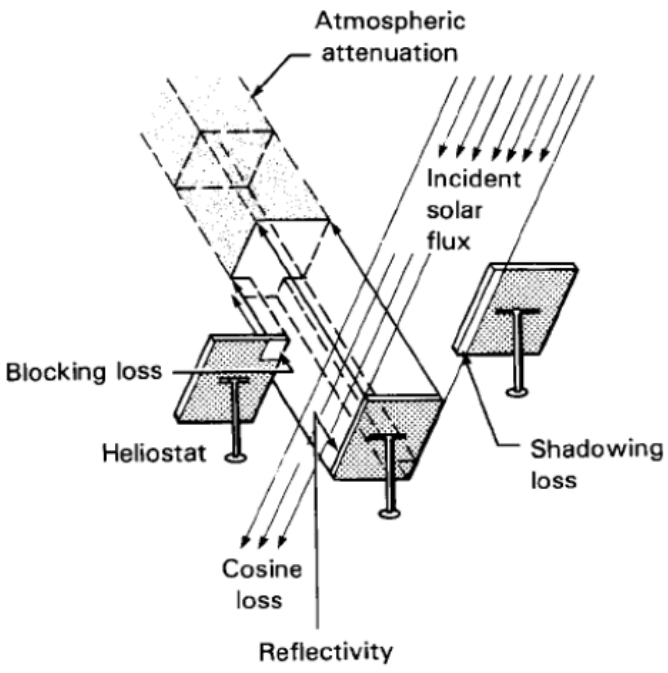

Figure 4-2 Collector Field Optical Processes (Falcone 1986)

The amount of insolation reflected by the heliostat is proportional to the amount of sunlight intercepted. The reflected power is proportional to the cosine of the angle (cosine effect) between the heliostat mirror normal and the incident sun rays; the ratio of the projected mirror area that is perpendicular to the sun's rays to the total area of the heliostat determines the magnitude of the cosine effect. The heliostat is oriented so that the incident sunlight is reflected onto the receiver.

Not all the sunlight that leaves the heliostats reaches the vicinity of the receiver. Some of the energy is scattered and absorbed by the atmosphere; this effect is referred to as the attenuation loss. A good visibility day will have a small percentage of energy loss per kilometer. The losses increase when water vapor or aerosol content in the atmosphere is high.

The efficiency of the solar field changes every hour of the year depending on the sun position. For the model, the values have been calculated for a CSP plant in a similar location using the System Advisor Model (SAM) by NREL, which is a performance and financial model designed to facilitate

decision making for people involved in the renewable energy industry (NREL, System Advisory Model (SAM) 2007).

ρ_{REC} is the performance of the receiver as defined below in constraint (2).

Constraint (2). Receiver

$$Q_{TS}(h) = Q_{SF}(h) * \rho_{REC}$$

Heat collected in the receiver at every hour ($Q_{TS}(h)$) is equal to the heat received in the solar field ($Q_{SF}(h)$) modified by the performance of the solar receiver.

ρ_{REC} is the performance of the solar receiver. Subsystem performance for different receiver configurations is the result of a variety of design tradeoffs among several loss mechanisms. These losses, shown schematically in Figure 4-3.

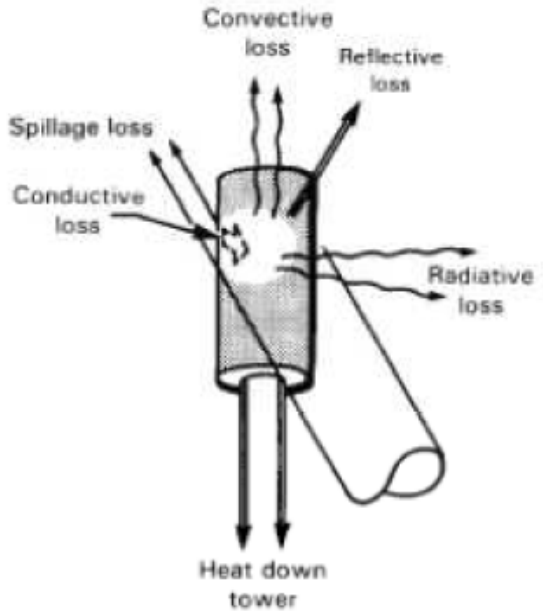

Figure 4-3 Receiver losses Processes (Falcone 1986)

Spillage: the energy reflected by the heliostat field, after accounting for atmospheric absorption between heliostat and receiver, which is not intercepted by an absorber surface containing the receiver heat transport fluid, or re-reflected or radiated from an intermediate surface to that absorber

surface. Spillage may be considered either a collector subsystem loss or a receiver subsystem loss. Spillage can miss the receiver entirely, or merely fall outside the absorber surface of the receiver. It may result from receiver sizing tradeoffs or heliostat aiming errors. The receiver is typically designed to keep overall spillage less than five percent of the reflected light reaching the vicinity of the receiver. For a well-designed plant, we are assuming an average spillage loss of 5% for the whole solar field (Falcone 1986).

Reflection: the radiant energy from the heliostat field scattered from the receiver surface and escaping from the receiver. High absorptivity paint is used on the absorber surfaces to minimize reflective loss. Reflection loss is five percent or less with a freshly-painted absorber surface, but may increase during service because of degradation of the coating. For the considered plant the reflection loss at design point is assumed at 5% (Falcone 1986).

Convection: the thermal energy lost in heating the air adjacent to the receiver. It is a combination of free (thermally driven) and forced (wind driven) convection. For a well-designed plant, the convection loss at design point should not be higher than 1.5% of the energy at the receiver (after reflection losses) (Falcone 1986).

Radiation: the thermal energy lost by infrared and visible light emission due to the high temperature of the receiver. Both the radiative and convective losses are a function of the temperature of the receiver and its configuration (external). For a well-designed plant the radiation loss at design point should be around 3% of the energy at the receiver (after reflection losses) (Falcone 1986).

Conduction: the thermal energy lost through the insulating surfaces and structural members. This loss is less than one percent (0.5%) for a well-insulated receiver (Falcone 1986).

Accordingly, the total performance of the receiver is calculated in Table 4-1. Note that this efficiency is slightly lower than the one considered by some authors (Ehrhart 2014). However, these values are considered more conservative.

Losses		**Efficiency**
Spillage	5%	95.0%
Reflection	5%	95.0%
Convection	1.50%	98.5%
Radiation	3%	97.0%
Conduction	0.50%	99.5%
Total efficiency		*86%*

Table 4-1 Receiver thermal efficiency

Constraint (3). Receiver design point

$$Q_{TS}(h) \leq 1{,}000\ \frac{W}{m^2} * A_{CSP} * \rho_{SF}(h)$$

The receiver design allows a maximum heat inflow defined by a normalized radiation of 1 kW/m^2 on the solar field (A_{CSP}). This is the design point of the receiver. Therefore, the receiver capacity is limited by the solar field area and the defined efficiency of the solar field.

Constraint (4). Thermal storage equations

$$S_{Clevel}(h) = S_{Clevel}(h-1) + Q_{TS}(h) - Q_{PB}(h)$$

The thermal storage level at every hour (S_{Clevel} (h)) is equal to the storage level at the precedent hour (S_{Clevel}(h-1)) modified positively by the thermal injection from the receive (Q_{TS}(h)) and negatively by the thermal extraction towards the power block (Q_{PB}(h)).

S_{Clevel} (h) is the level of thermal storage in hour h.

S_{Clevel} (h-1) is the level of thermal storage in hour h-1.

Q_{TS} is the injection of thermal energy in the storage from the solar field.

Q_{PB} is the extraction of thermal energy from the storage to be used for steam generation.

Constraint (5). CSP generation

$$P_{CSP}(h) = Q_{PB}(h) * \rho_{TS} * \rho_{Rankine}(h) - Auxiliary\ Loads(h)$$

The power generated by the CSP plant is the power generated by the thermal energy extracted from the thermal storage (Q_{PB}(h)) less the consumption of auxiliary power.

ρ_{TS} is the performance of the molten salts thermal storage. This performance has been assumed to be 98% based on ((Kolb 2011)and (Ehrhart 2014)).

$\rho_{Rankine}$ (h) is the performance of the Rankine cycle, which has been assumed to be that calculated by (Kolb 2011) (Figure 4-4). From those values a linear regression has been calculated to feed into model:

$$\rho_{Rankine} = -0.048 * T\ (℃) + 0.028 * Load(\%) + 39.76$$

Auxiliary loads (h) are the loads required to run the auxiliary services of the CSP plant. They have assumed to be those calculated by (Kolb 2011)(Figure 4-4) for a 100 MWe plant. From those values a linear regression has been calculated to feed the model:

$$Auxiliary\ loads = 44.84 * T\ (℃) + 37.93 * Load(\%) - 262.33$$

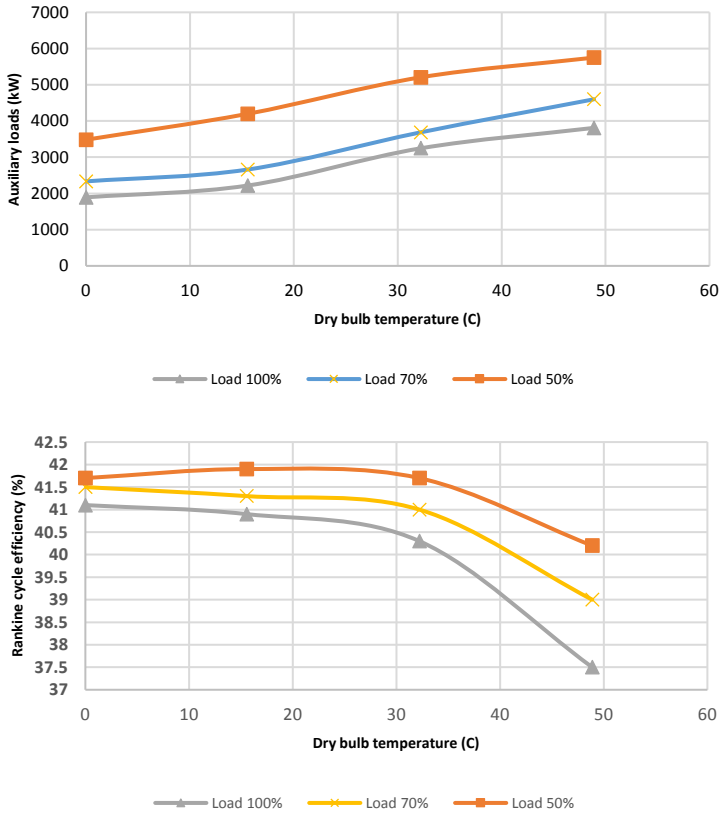

Figure 4-4 Auxiliary loads and Rankine cycle efficiency for a 100 MWe CSP plant with dry cooling (Kolb 2011)

The formulas above have been applied to each country, considering each measured annual average temperature and an average load of 75% for the CSP plants. From Table 4-2, which indicates the calculated values, it can be estimated with a high degree of accuracy that average values for all countries can be set at 41% for Rankine efficiency and 3.5% for an auxiliary loads percentage.

Country	Average temperature (C)	Rankine efficiency	Auxiliary loads percentage
Jordan	**18.8**	**41.0%**	**3.4%**
Egypt	**22.5**	**40.8%**	**3.6%**
KSA	**24.5**	**40.7%**	**3.7%**
UAE	**28.8**	**40.5%**	**3.9%**
Oman	**28.1**	**40.5%**	**3.8%**
Kuwait	**26.2**	**40.6%**	**3.8%**
Iraq	**22.9**	**40.8%**	**3.6%**
Yemen	**20.5**	**40.9%**	**3.5%**
Libya	**18.9**	**41.0%**	**3.4%**
Tunisia	**20.6**	**40.9%**	**3.5%**
Morocco	**14**	**41.2%**	**3.2%**
Algeria	**21**	**40.9%**	**3.5%**
Lebanon	**17**	**41.1%**	**3.3%**
Syria	**20**	**40.9%**	**3.5%**
Iran	**17.8**	**41.0%**	**3.4%**
Average		41.0%	3.5%

Table 4-2 Rankine efficiency and auxiliary loads calculation

Constraints Photovoltaics and Energy storage system

Constraint (6). Solar field generation

$$P_{DG}(h) + P_{DI}(h) \leq GHI(h) * A_{PV} * \rho_{Panel} * PR_{in}$$

The energy generated by the PV solar field at every hour, including the energy directly injected into the grid ($P_{DG}(h)$) and the energy that is sent to the battery storage ($P_{DI}(h)$) is equal or lower than the power generated by the solar panels using the radiation (GHI(h)).

ρ_{Panel} is the efficiency of the solar panels. This efficiency has been estimated from the last updates and forecast by NREL, according to Figure 4-5 (Feldman D. 2016). The selected value for the model has been 18%, which is a reasonable, and even conservative, value for Thin-Film and Crystalline Si Cells.

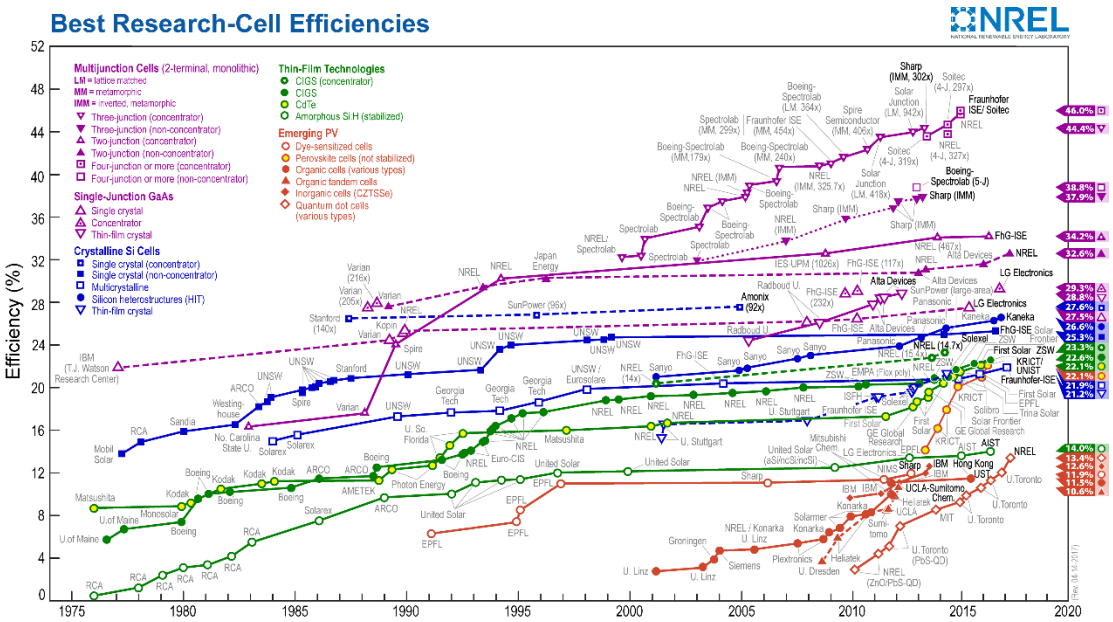

Figure 4-5 PV cells efficiencies from 1976 to 2017 (Source: NREL)

PR_{in} is the performance ratio of the solar field. The performance ratio (PR) is defined in IEC 61724 and is a metric commonly used to measure solar PV plant performance for acceptance and operations testing. The PR measures how effectively the plant converts sunlight collected by the PV panels into AC energy delivered to the off-taker relative to what would be expected from the panel nameplate rating. Although this metric quantifies the overall effect of losses due several factors including inverter inefficiency, in our case the inverter inefficiency has been treated separately. The value of PR_{in} has been estimated in 91% according to the reference (NREL 2013).

Constraint (7). BESS

$$S_{Plevel}(h) = S_{Plevel}(h-1) + P_{DI}(h) - P_{DO}(h)$$

The energy stored in batteries at every hour (S_{Plevel} (h)) is equal to the storage level at the precedent hour (S_{Plevel}(h-1)) modified positively by the energy injected from the solar field (P_{DI}(h)) and negatively by the energy sent to the grid (P_{DO}(h)).

S_{Plevel} (h) is the level of battery storage in hour h.

S_{Plevel} (h-1) is the level of battery storage in hour h-1.

Constraint (8). PV generation

$$P_{PV}(h) = [P_{DG}(h) + P_{DO}(h)] * \rho_{BESS} * \rho_{Inverter} * (1 - PV\ Auxiliary\ Loads)$$

The total power injected into the grid at every hour (P_{PV}(h)) is the sum of energy directly from the PV solar field (P_{DG}(h)) and the energy from the energy storage (P_{DO}(h)) less the auxiliary consumption.

ρ_{BESS} is the performance of the efficiency of the battery storage system based on its round-trip efficiency. According to recent studies (Patsiosa 2016), battery degradation and round-trip efficiency is highly dependent on the battery state of charge (SoC). Higher SoC floating points were shown to increase the rate of battery degradation, while lower SoC floating points were shown to decrease system efficiency due to higher polarization losses in the battery. The energy balance in batteries shows that the majority of losses (59–67%) are originated in the power converter. However, in the system modeled in this study, those losses are not included as they are accounted in the inverter with the PV plant. Therefore, the BESS model just considers the round-trip efficiency and auxiliaries, in a single value of 88%. The round-trip efficiency is estimated from Figure 4-6 in a conservative average value of 90%, while the auxiliaries are estimated to be just 2% of the battery energy on average (Patsiosa 2016).

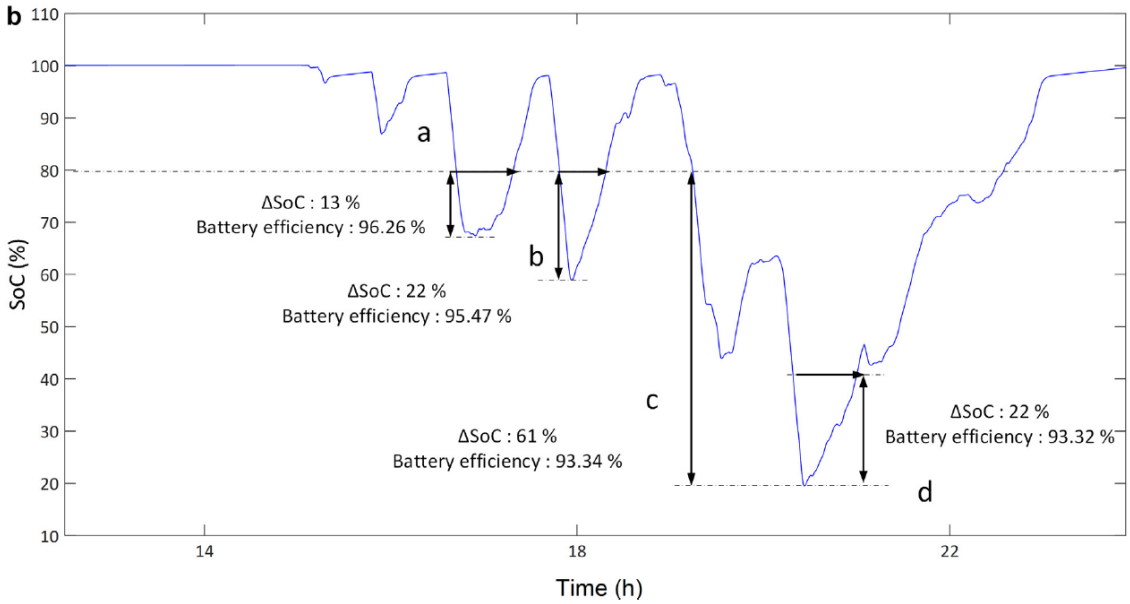

Figure 4-6 Round trip efficiency (battery efficiency) vs state of charge (SoC) (Patsiosa 2016)

$\rho_{Inverter}$ is the efficiency of the inverter system. This system applies to both PV and BESS output. Inverter manufacturer lists the efficiency of the conversion of DC power to AC power in the 92-95% range. Although peak efficiencies are not maintained over the whole range of operation, inverters operate at greater than 90% over much of the range (Vignola, Mavromatakis and Krumsick 2008). For the model in this study the efficiency of inverters has been estimated to be 93%.

PV Auxiliary loads is the percentage of the PV generation that is consumed by the auxiliaries and include transformer losses, and have been estimated at 2%.

Constraints on power demand coverage

Constraint (9). Demand-supply balance

$$D(h) = P_{CSP}(h) + P_{PV}(h) + Unserved\ (h)$$

The demand at every hour (D(h)) has to be satisfied by the energy from the CSP ($P_{CSP}(h)$) and the energy from the PV ($P_{PV}(h)$). The demand that cannot be satisfied is unserved (Unserved(h)).

Unserved (h) is the amount of energy that is not covered by the generation by either CSP or PV. The value of Unserved Energy (USE) is the summation of the expected number of megawatt hours of load that will not be served in a given moment as a result of demand exceeding the available capacity across all hours (NERC 2016). In the case of this study, this cost will also include the need to have an additional baseload generation source just for hours when the generation with solar cannot be achieved or is too expensive. The value fix for USE is economically estimated in around US$1,000/MWh. This value tries to minimize the amount of energy that is not generated by solar to evaluate what would be the feasibility and cost of having solar as a base load with the maximum reliability of the service.

4.3.2. Objective function

The objective function represents the total cost of generation throughout one year, and it is the value that will be minimized, subject to the constraints indicated above. The function is driven by the economic parameters and intends to minimize the cost of running the complete system for one year, including annual CAPEX amortization and annual OPEX.

Function objective (10). Total system cost.

$$Min\ Cost = [(A_{CSP} * CSP_{SF} + A_{PV} * PV_{SF} + S_{CSP} * CSP_{ST} + B_{CSP} * CSP_{PB} + B_{PV} * PV_{PB} + R_{CSP} * CSP_{REC}) * CRF_{25} + S_{PV} * PV_{ST} * CRF_{10}] + (A_{CSP} * CSP_{SFx} + A_{PV} * PV_{SFx} + S_{CSP} * CSP_{STx} + S_{PV} * PV_{STx} + B_{CSP} * CSP_{PBx} + B_{PV} * PV_{PBx} + R_{CSP} * CSP_{RECx}) + \sum_{1}^{8760} Unserved\ (h) * \text{USE}$$

A_{CSP} is the total area of solar field for CSP plants in m^2.

A_{PV} is the total area of PV panels for PV plants in m^2.

S_{CSP} is the size of the thermal energy storage for CSP plants in MWh_{th}.

S_{PV} is the size of BESS for PV plants in MWh.

B_{CSP} is the nominal power of CSP in MWe gross.

B_{PV} is the nominal power of PV plants in MWe gross.

R_{CSP} is the nominal size of the CSP receiver in MW_{th}.

CSP_{SF} is the cost of solar field for CSP in the different scenarios. This value is explained and calculated in Section 5.3.

PV_{SF} is the cost of solar panels for PV in the different scenarios. This value is explained and calculated in Section 5.3.

CSP_{ST} is the cost of thermal storage for CSP in the different scenarios. This value is explained and calculated in Section 5.3.

PV_{ST} is the cost of BESS for PV in the different scenarios. This value is explained and calculated in Section 5.3.

CSP_{PB} is the cost of power block for CSP in the different scenarios. This value is explained and calculated in Section 5.3.

PV_{PB} is the cost of power block for PV in the different scenarios. This value is explained and calculated in Section 5.3.

CRF_{10} is the capital recovery factor for a return period of 10 years. This value is calculated following the assumptions detailed in section 5.4.

CRF_{25} is the capital recovery factor for a return period of 25 years. This value is calculated following the assumptions detailed in section 5.4.

CSP_{SFx}, PV_{SFx}, CSP_{STx}, PV_{STx}, CSP_{PBx}, CSP_{PBx}, PV_{PBx}, CSP_{RECx} are the annual cost of operation and maintenance for each element of the structure. These values have been estimated in 1% of investment costs.

USE is the cost of the unserved energy, equal to US$1,000/MWh.

4.4. Scenario definition

The study has been carried out for three different technology cost scenarios, each of which corresponds to a different time scenario. Being CSP and PV+BESS two fast evolving technologies, the expected technology changes in the coming years need to be taken into consideration. Reviewing the existing literature and other recent sources of information, there is a notable consensus that both technologies will dramatically change during the next 10-15 years. These changes will likely come in the form of technology improvements which in turn will lead to cost improvements that will drastically reduce the installation costs in this period (2018-2033). Therefore, it seems reasonable that the study is performed in four scenarios spread out through that period.

The scenarios considered for the study set four points in time based on the current cost forecasts of the different technologies. On that basis, the model is run and the results are obtained. Results are then compared to the different countries for each scenario and two typical cases (countries) are selected. For those two countries, a more detailed analysis is carried out in order to compare the results across the different scenarios. Figure 4-7 depicts the general analytical framework for this study.

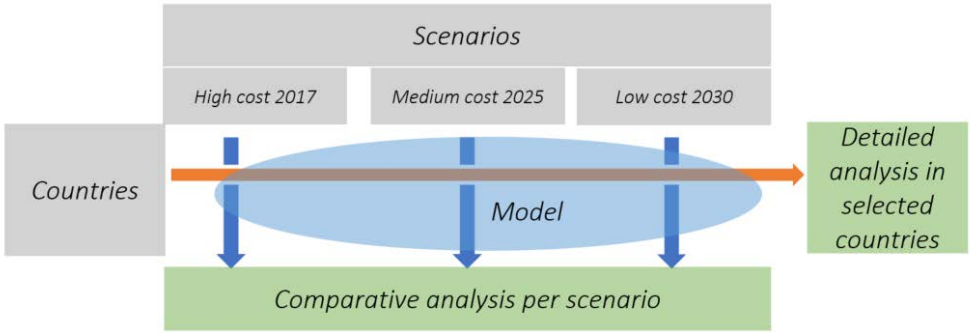

Figure 4-7 Results analysis diagram

5. Assumptions and data

5.1. Solar radiation

The solar radiation for CSP and PV plants, DNI and GHI respectively, have been obtained from reliable databases (Meteosat, EUMETSAT, ECMWF, NOAA, Solargis) in different locations for each country. The database provides with hourly data of DNI, GHI and temperature for several geographic coordinates in each country. To select the point for carrying out the analysis, the annual value has been calculated for each parameter (DNI and GHI) and each country, using the respective locations. The location for the analysis in each country has been selected based on the location of the closest value to this average. As an example, Morocco the database provides with DNI and GHI data for four geographic locations (Figure 5-1). The values for both types of radiation are analyzed and the selected location is the one whose value is closest to the average.

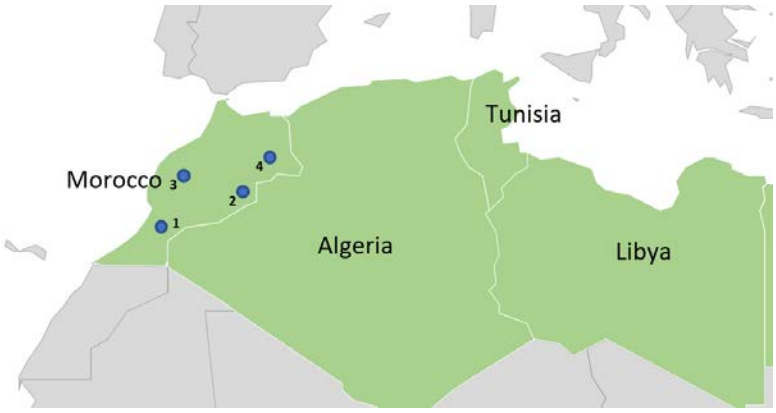

Figure 5-1 Data locations in Morocco

Analyzing the data for DNI, the selected location in this case is Morocco 4 (Figure 5-2).

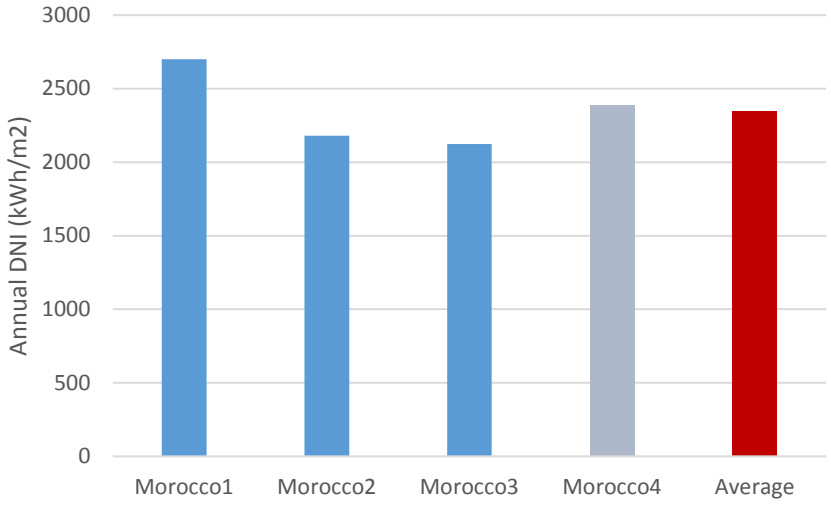

Figure 5-2 DNI data in different locations in Morocco (Meteosat, EUMETSAT, ECMWF, NOAA, Solargis)

However, for the GHI data, the database provides the data for those same four locations (Figure 5-3), but the closest to the average is Morocco 2.

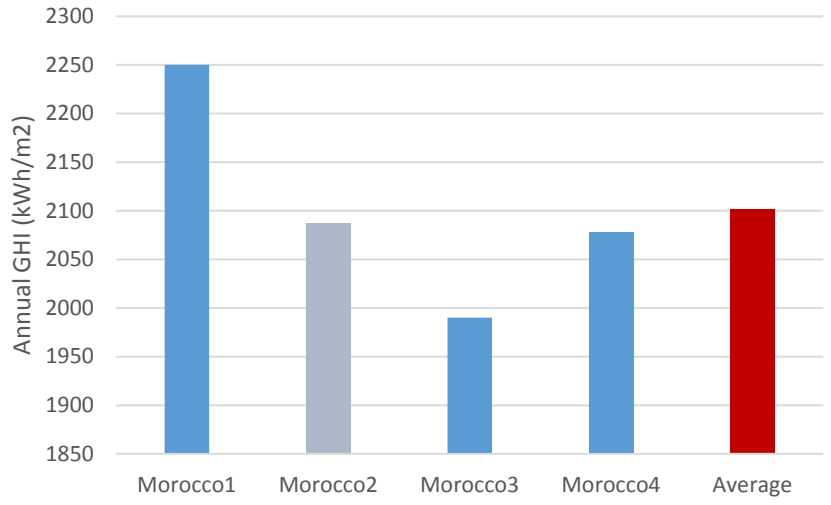

Figure 5-3 GHI data in different locations in Morocco (Meteosat, EUMETSAT, ECMWF, NOAA, Solargis)

Therefore, the model will use Morocco4 for DNI data (CSP modeling) and Morocco2 for GHI data (PV modeling). This strategy allows a more realistic approach to the study, as it is supposed that the plants will be optimally located with the best resources located across the country, which would be explicitly selected for one or another technology.

Following this rationale, one location has been selected in each country for DNI and for GHI. Figure 5-4 shows the selected locations for the analysis of DNI (CSP) and GHI (PV). In some cases, the locations coincide.

	DNI		GHI	
	Latitude	Longitude	Latitude	Longitude
Jordan	30.63	36.35	29.79	36.47
Egypt	25.88	31.66	25.88	31.66
KSA	25.28	39.53	26.51	39.53
UAE	23	53.37	23	53.37
Oman	19.68	56.57	19.68	56.57
Kuwait	29.32	47.17	28.87	47.9
Iraq	35.35	42.78	31.09	44.01
Yemen	14.54	45.03	14.54	45.03
Libya	31.39	12.72	26.03	18.57
Tunisia	32.9	10.74	33.06	8.81
Morocco	33	-3.26	31.42	-4.53
Algeria	31.54	2.88	28.22	-0.77
Lebanon	34.33	36.4	33.98	36.13
Syria	33.72	38.68	32.84	37.06
Iran	30.79	53.68	30.79	53.68

Table 5-1 Coordinates of selected points in each country

Figure 5-4 Location of DNI points of analysis in each country (for CSP plants)

Figure 5-5 Location of GHI points of analysis in each country (for PV plants)

The selected annual DNI and GHI values, and ratio between both values for each country are indicated in Table 5-3, Figure 5-6 and Figure 5-7.

	DNI	GHI	DNI/GHI
Lebanon	2430	2044	1.19
Morocco	2389	2087	1.14
Jordan	2540	2244	1.13
Syria	2258	2094	1.08
Tunisia	2041	2006	1.02
Yemen	2499	2466	1.01
Iran	2122	2106	1.01
Libya	2191	2214	0.99
Algeria	2090	2134	0.98
Egypt	2245	2297	0.98
KSA	2217	2283	0.97
Oman	2105	2313	0.91
Iraq	1827	2027	0.90
Kuwait	1786	2031	0.88
UAE	1968	2240	0.88

Table 5-2 Values of annual radiation (DNI and GHI) for each location (Meteosat, EUMETSAT, ECMWF, NOAA, Solargis)

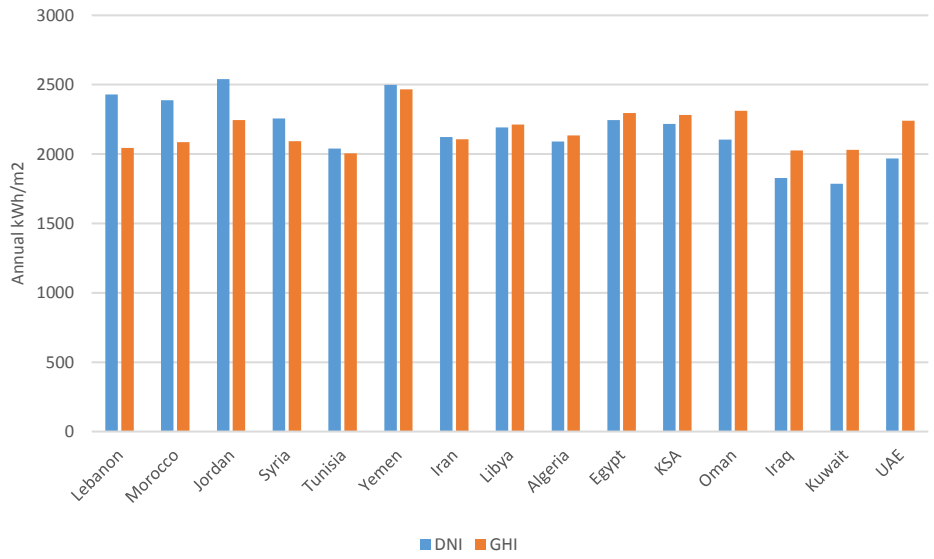

Figure 5-6 Values of DNI and GHI in considered in each country and relation between values (Meteosat, EUMETSAT, ECMWF, NOAA, Solargis)

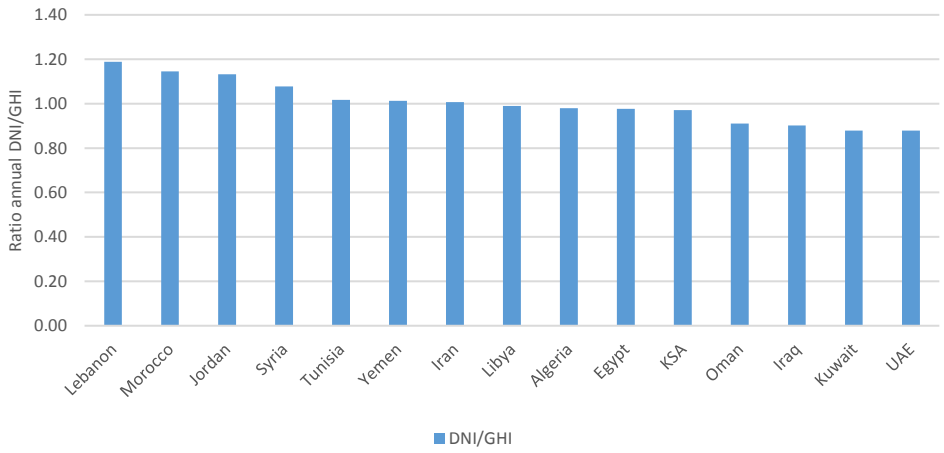

Figure 5-7 Ration between annual DNI and GHI in each country

As depicted in Figure 5-7 the highest DNI/GHI ratio correspond to Lebanon, Morocco and Jordan, where it is supposed that CSP technology would be a better fit than PV. On the contrary, the lowest ratios correspond to Oman, Iraq, Kuwait and UAE, where PV would theoretically have better performance than CSP.

5.2. Demand profile

The demand profile for each country has been obtained from real data from 2016[4]. Table 5-3 includes the demand profile of the fifteen countries analyzed within this study. As it can be observed in the profiles, there are basically three types of profiles:

a) flat profiles shown by countries in the Gulf sub-region: KSA, UAE, Oman, Iraq and Kuwait;
b) profiles with a clear peak demand in evening hours, mainly in North Africa: Egypt, Yemen, Libya, Tunisia, Morocco, Algeria, Lebanon and Syria;
c) profiles with a peak around noon: Jordan and Iran.

The 8,760-hour demand data series for each country has been considered and included in the model. From the point of view of the technology mix, it does not matter the absolute value of the peak demand, but the distribution of demand throughout the year. For that reason, the peak demand has been normalized to 100 MW for all the countries. The model calculates the optimal generation mix of CSP/PV that satisfies that demand. Capacity results can be later extrapolated proportionally to any other peak demand requirement.

5.3. Cost data for solar technologies

As mentioned above, one of the most critical parameters of this study when analyzing is the cost of the two solar technologies considered and each of their components. Those costs need to be accurately estimated to obtain reliable results. In rapidly evolving technologies, as solar and batteries, that estimation is even more critical.

[4] Demand data from World Bank and Arab League databases.

In order to define a suitable cost structure for the model, the study has set a proper decomposition of the respective solar technologies. That cost structure defines the cost of homogeneous and scalable parts of each technology. Furthermore, the elements of the structure allow establishing a cost evolution in different time scenarios for each of these elements. The cost structure defined for the model includes four elements for CSP and three elements for PV described in section 4.1:

- For Concentrated Solar Power: Component CSP-A, Solar field; Component CSP-B, Receiver; Component CSP-C, Thermal storage; and Component CSP-D, Power block.
- For Solar Photovoltaics (PV): Component PV-A, Solar field; Component PV-B, Balance of Plant; and Component PV-C, Battery Energy Storage System (BESS).

Table 5-3 Demand profiles of countries included in the study (World Bank and Arab League databases)

Concentrated Solar Power cost structure

The CSP technology has been divided into four main elements: solar field, receiver, thermal storage and power block. Table 5-5 includes the database for the cost structure of CSP. The plant has been sub-divided into different items and each item has been allocated to its respective element. Those values are always referred to a single unit per element (m^2 for solar field, MWh_{th} for TES and MWe for power block).

The database indicated in Table 5-5 has been built upon data from existing projects. The baseline for 2017 has been constructed with cost information from real projects and has been verified with real projects found in the literature and other publicly available information. For 2030, different assumptions have been considered following the reference indicated in Figure 5-9 (Feldman D. 2016). As a verification example, the cost of a CSP plant of 100 MWe with, 1,100,000 m^2 of solar field, 600 MW_{th} of receiver and 10 hours storage (2,430 MWh_{th} of TES) has been considered in the three scenarios. Values are indicated in the table.

	High cost 2017 [5]	***Medium cost 2025*** [6]	***Low cost 2030*** [7]
Solar Field (CSP-A)= CSP_{SF} (US$/$m^2$)	200	160	120
Receiver (CSP-B)=CSP_{RE}(US$/$MW_{th}$)	80,000	60,000	40,000
Storage (CSP-C)=CSP_{ST} (US$/$MWh_{th}$)	24,000	18,000	12,000
BOP (CSP-D)=CSP_{PB} (US$/MWe)	2,100,000	1,950,000	1,800,000
CSP Total cost (verification CSP plant)	$536,320,000	$450,740,000	$365,160,000
Reduction in installed costs		84%	68%

Table 5-4 Scenarios for cost structure of CSP plants. Example of validation of cost structure evolution

[5] Values according to Table 5-5

[6] Values interpolated from Table 5-5

[7] Values according to Table 5-5

The cost structure defined for this study in the three scenarios is represented in Figure 5-8.

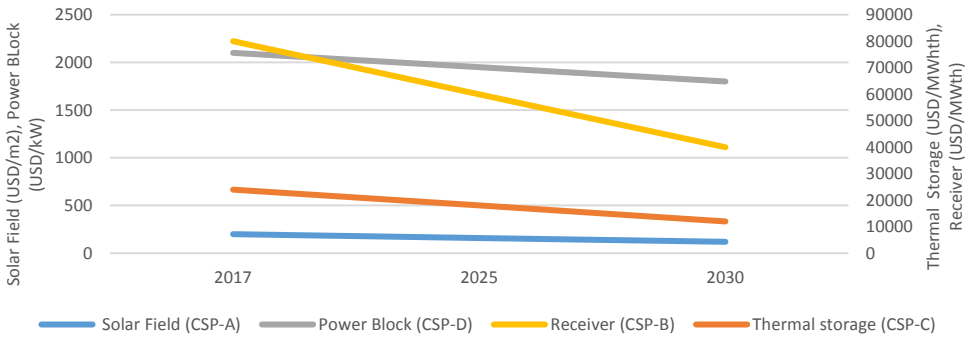

Figure 5-8 Evolution of cost structure for CSP

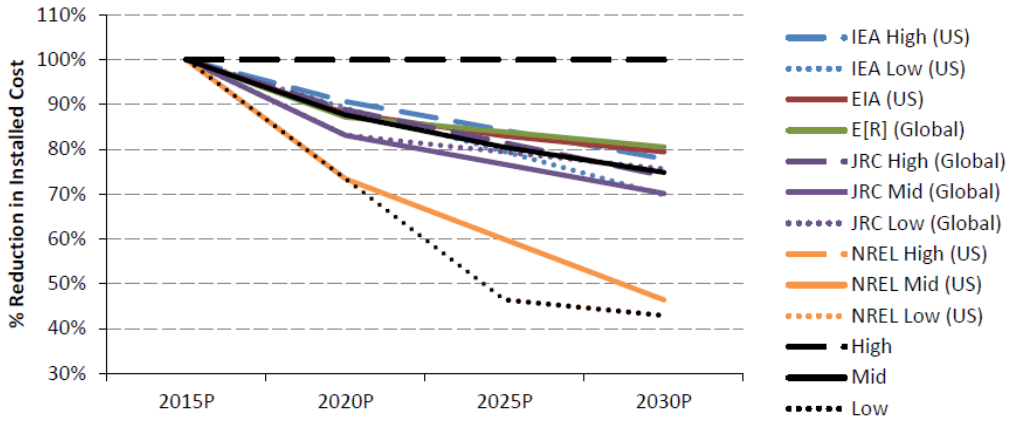

Figure 5-9 Projected CSP system prices, 2015–2030 ((Feldman D. 2016)

Equipment	***Solar field (US$/m2)***		***Receiver (US$/MWth)***		***TES (US$/MWhth)***		***Power Block (US$/MWe)***	
	2017	**2030**	**2017**	**2030**	**2017**	**2030**	**2017**	**2030**
Heliostats field	$102.6	$51.0						
Receiver			$71,000	$35,000				
Tower	$11.79	$5.64						
Electrical and control	$11.74	$12.49					$250,000	$220,000
TES system					$10,500	$4,000		
Salts					$10,300	$6,200		
Power Block and BOP							$500,000	$430,000
Piping							$120,000	$89,000
General activities								
Civil Works	$15.48	$14.70					$166,000	$158,000
Mechanical erection and structures	$9.46	$8.52					$199,000.00	$178,000.00
Piping and insulation							$193,000	$162,000
Electrical and control erection	$3.54	$2.62					$77,000	$55,000
Commissioning	$2.38	$1.90					$50,000	$39,000
Services								
Engineering and overheads	$10.22	$6.71			0	0	$215,000	$140,000
Net Cost	**$167**	**$103**	**$71,000**	**$35,000**	**$20,800**	**$10,200**	**$1,770,000**	**$1,471,000**
Risks (5%)	$8.36	$5.18	$3,550	$1,750	$1,040	$510	$88,500	$73,550

EPC Margin (10%)	$17.56	$10.88	$7,455.00	$3,675.00	$2,184	$1,071	$185,850	$154,455
Contingency (2%)	$3.86	$2.39	$1,640	$808	$480	$235	$40,887	$33,980
Total Cost	**$196**	**$122**	**$83,645**	**$41,233**	**$24,504**	**$12,016**	**$2,085,237**	**$1,732,985**

Table 5-5 Cost structure CSP plant

PV + BESS cost structure

The PV plant has been divided in three main elements: solar field, battery energy storage system (BESS) and power block. The dramatic drop of PV plants costs in the last years makes complicated to set a baseline for this type of plants. For the BESS component, the absence of public itemized information about real projects presents a major obstacle for estimating the current costs and future trends. However, there are recent studies that have compiled valuable information to estimate those costs.

The values for solar panels and power block are obtained from the most recent studies that have collected updated information from existing projects. Those studies (Creara 2017) show that the price of modules would be around US$0.45/Wp, which means around US$90/$m^2$. The fact that this value has been set as a long-term objective in other recent studies (Feldman D. 2016) indicates the degree of uncertainty of cost for this technology in the forthcoming years. Therefore, for the scenarios of medium and low costs (2025 and 2030) similar costs have been considered following current forecast (Feldman D. 2016). At this point, we have to assume that further reduction would be hardly justifiable with such low current costs.

For the power block, the study assumes US$0.8/Wp as per the reference (Figure 5-10) and no significant improvement is expected in this cost over the coming years.

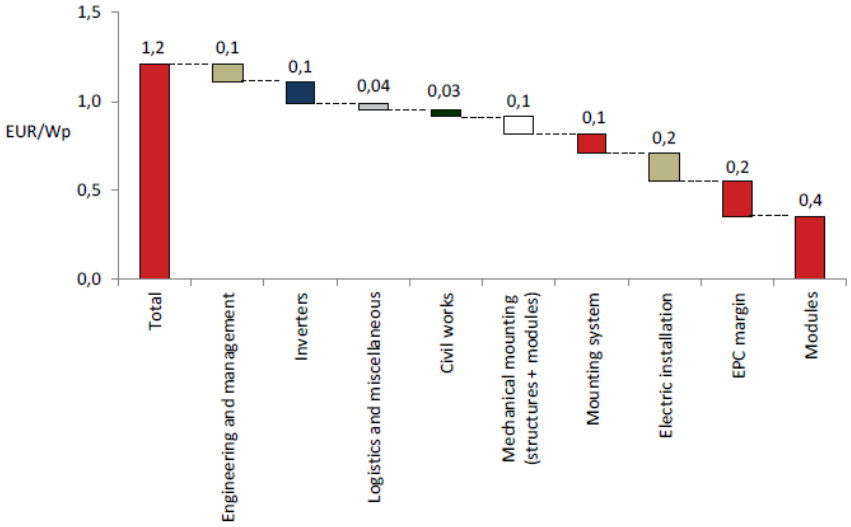

Figure 5-10 Current PV system prices, 2014 (Creara 2017)

For the BESS, the study has analyzed recent studies (Feldman D. 2016) (Patsiosa 2016). Figure 5-11 shows the expected installation cost evolution for BESS. The study, therefore, has considered costs linked to this study.

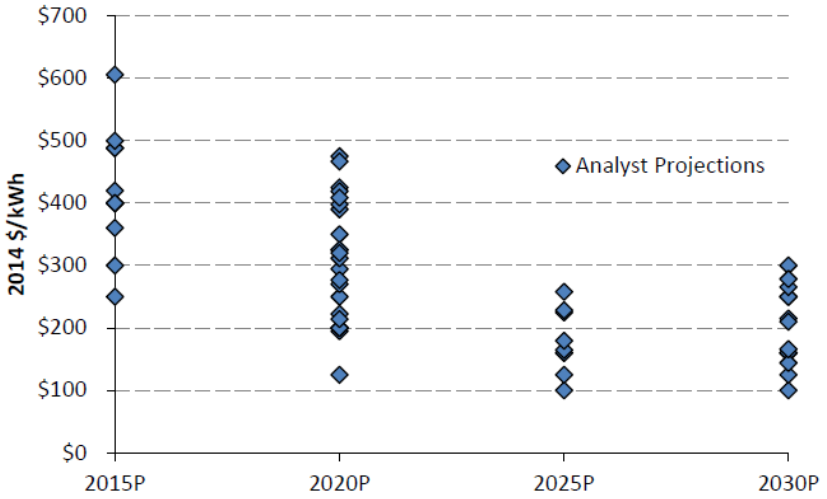

Figure 5-11 Price estimates for Li-ion battery pack, 2015–2030 (Feldman D. 2016)

Considering the data analysis described above, the cost structure defined for PV+BESS in the three scenarios are represented in Figure 5-8.

	High cost 2017 [8]	Medium cost 2025 [9]	Low cost 2030 [10]
Solar Field (PV-A)= PV_{SF} (US$/m^2)	90	90	90
Storage (PV-B)=PV_{ST} (US$/MWh$_e$)	500,000	250,000	150,000
BOP (PV-C)=PV_{PB} (US$/MWe)	900,000	900,000	900,000

Table 5-6 Scenarios of cost structure for PV plant

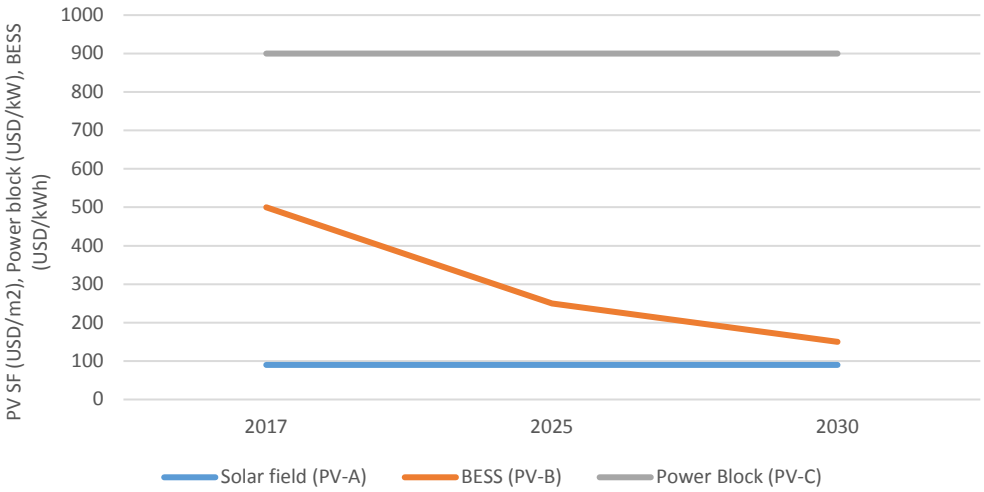

Figure 5-12 Evolution of cost structure for PV system (including BESS)

5.4. Economic parameters

The analysis carried out in this study includes the technical aspect of supplying a defined demand through solar energy and its economic implications. As with any other economic analysis, it is required to set some specific economic parameters to represent existing financing conditions, amortization periods, etc. The parameters have been estimated following internationally accepted benchmark values.

[8] Values according to Table 5-5

[9] Values interpolated from Table 5-5

[10] Values according to Table 5-5

Weighted Average Cost of Capital

The Weighted Average Cost of Capital (WACC) is a financial parameter used to measure the cost of capital for a defined investment. In any investment, the cost of financing the capital is a reasonably logical price tag to put on the investment, so WACC is used to determine the discount rate used.

There are two main sources to raise money for an investment: equity and debt. WACC is the weighted average of the costs of these two sources of financing.

In the study, the baseline WACC is estimated at fairly commercial rates at 8%.

Levelized cost of electricity

The economic analysis will be mainly based on the levelized cost of electricity (LCOE) calculated for each technology and for the correspondent mix. The LCOE will be calculated following the general definition (IEA 2015) but adapted to a single year calculation.

$$LCOE = \frac{\sum_t((Investment_t + O\&M_t + Carbon_t + Decommissioning_t) * (1+r)^{-t}}{\sum_t(Electricity_t * (1+r)^{-t})}$$

For a single year calculation, and considering that Carbon=0 because we are dealing with solar energy and not considering decommissioning costs, the calculation will be done according to the formula:

$$LCOE_t = \frac{Investment_t * CRF + O\&M_t}{Electricity_{\ t}}$$

CRF is the cost recovery factor defined as:

$$CRF = \frac{i * (1+i)^n}{(1+i)^n - 1}$$

i is the discount rate; and n is the economic lifetime of assets.

For investments, the study considers that the discount rate is equal to the weighted average cost of capital (WACC). Since the type of investment are power plants, the study estimates an economic lifetime for the assets of 25 years, except for the BESS whose economic lifetime is estimated in 10 years.

Taking into account the cost structure defined for both solar technologies, the annual LCOE calculation would be:

$$LCOE = \frac{([(A_{CSP}*CSP_{SF}+A_{PV}*PV_{SF}+S_{CSP}*CSP_{ST}+B_{CSP}*CSP_{PB}+B_{PV}*PV_{PB}+R_{CSP}*CSP_{REC})*CRF_{25}+S_{PV}*PV_{ST}*CRF_{10}]}{Annual\ Electricity_{\ CSP}+Annual\ Electricity_{\ PV}} +$$

$$+\frac{(A_{CSP}*CSP_{SFx}+A_{PV}*PV_{SFx}+S_{CSP}*CSP_{STx}+S_{PV}*PV_{STx}+B_{CSP}*CSP_{PBx}+B_{PV}*PV_{PBx}+R_{CSP}*CSP_{RECx})}{Annual\ Electricity_{\ CSP}+Annual\ Electricity_{\ PV}}$$

A_{CSP} is the total area of solar field for CSP plants in m^2.

A_{PV} is the total area of PV panels for PV plants in m^2.

S_{CSP} is the size of the thermal energy storage for CSP plants in MWh_{th}.

S_{PV} is the size of BESS for PV plants in MWh.

B_{CSP} is the nominal power of CSP in MWe gross.

B_{PV} is the nominal power of PV plants in MWe gross.

R_{CSP} is the nominal size of the CSP receiver in MWh_{th}.

CRF_{25} is the cost recovery factor considering a lifetime of the asset of 25 years: $CRF = \frac{i*(1+i)^{25}}{(1+i)^{25}-1}$

CRF_{10} is the cost recovery factor considering a lifetime of the asset of 10 years: $CRF = \frac{i*(1+i)^{10}}{(1+i)^{10}-1}$

For the operation and maintenance (CSP_{SFx}, CSP_{STx}, CSP_{PBx}, CSP_{RECx}, PV_{SFx}, PV_{STx}, PV_{PBx}), the costs are estimated as an annual percentage of investment costs. The selected percentages are 1% for all parameters except for power block of PV plants (0.5%).

5.5. Other assumptions

Other assumptions of the model used in this study are:

- The model assumes that there are no transmission losses in the system. The calculation is based on a supply-demand balance. However, as this balance is based in relative amounts over a fix 100 MW of peak demand, this simplification does not invalidate the results.
- The model does not incorporate any other generation source. It intends just to satisfy the required demand with the solar energy, either directly or after storage.
- The time resolution of the model is hourly. All sub-hourly phenomena that are normally involved in any system level dispatch, as stability and/or sub-hourly variability, are not considered in the model.
- The model assumes each country is electrically independent and, therefore, there is not electricity exchange among them. Although this is not exactly true, the reality is that countries in this region are quite independent.
- The model is run for specific scenario/year and cost calculations are based on annual balances.

6. Analysis base-case for the region

This chapter describes the results of the model, summarizing the findings from the different scenarios that have been run. The analysis is conducted for fifteen countries, extracting conclusions about the relationships between the different variables monitored and how they evolve with the

scenarios. Based on that multi-country analysis, we will select two specific countries that characterize different behaviors. Results will be analyzed in more depth for those countries.

Firstly, the analysis focuses on explaining the relative amount of each type of generation (CSP and PV with respective storages) that is optimally installed in each scenario. This share is expressed in two parameters: installed capacity and total energy generation. Different ratios have been defined to facilitate the comparison in such varied environment. At the same time, the energy that is not economically possible to serve will be quantified and compared in different countries and time scenarios.

Secondly, according to the results obtained above the analysis intends to extract some correlations with the boundary conditions, mainly radiation values. Those correlations, if exist, will allow to set the predominant factor for deciding the best technology in each location and cost scenario.

Finally, the analysis sets general conclusions from the study and tries to determine the foreseeable future for solar generation, its viability, adequacy and economic implications for the countries in the region.

6.1. Total installed capacity

According to the results, the total installed capacity (Figure 6-1) will be progressively reduced as the technologies costs go down, in particular that of battery storage. With lower storage costs, the model prioritizes the installation of storage to better manage the solar generation, reducing the extra generation capacity needed to supply demand.

Figure 6-1 also indicates how the lower cost of generation and storage technologies in 2020 and 2030 will optimize the installed capacity in order to cover the demand. As stated in the assumptions, the demand has been normalized to a 100 MW peak in all countries. While in scenarios 2017 and 2020 all countries show an installed capacity above 100 MW (except Syria and Iraq), in the low-cost scenario 2030, many of the countries have an installed capacity below or just limiting the 100

MW. In those cases, there is unserved demand for some hours during the day. Considering these are very few hours, the model decides that it is more favorable for system cost to leave this energy as unserved instead of installing excess capacity that will only be used a handful of hours a year.

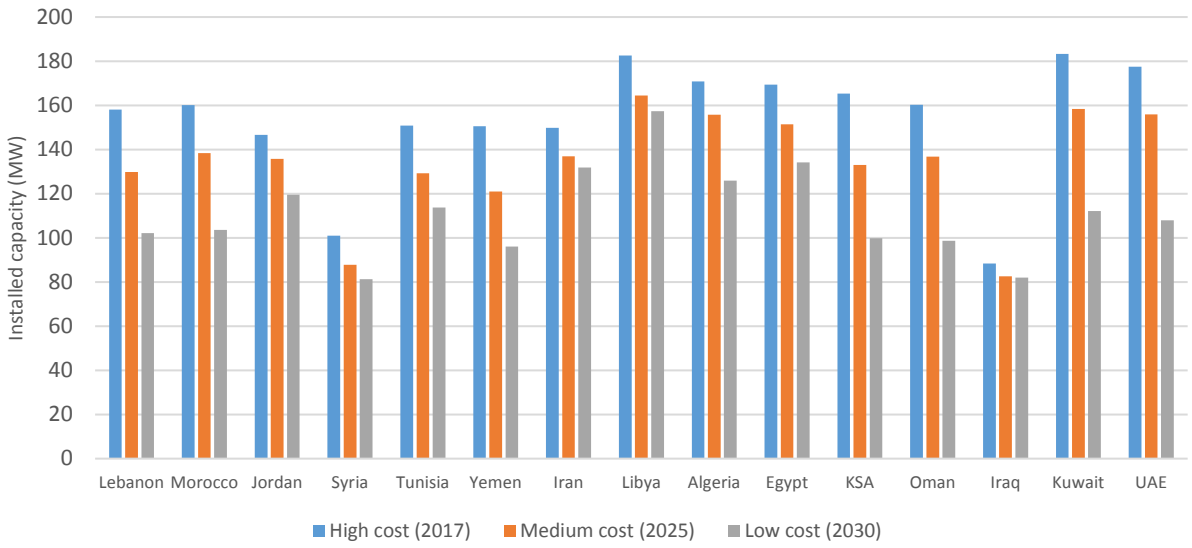

Figure 6-1 Total installed capacity in each country in the different scenarios

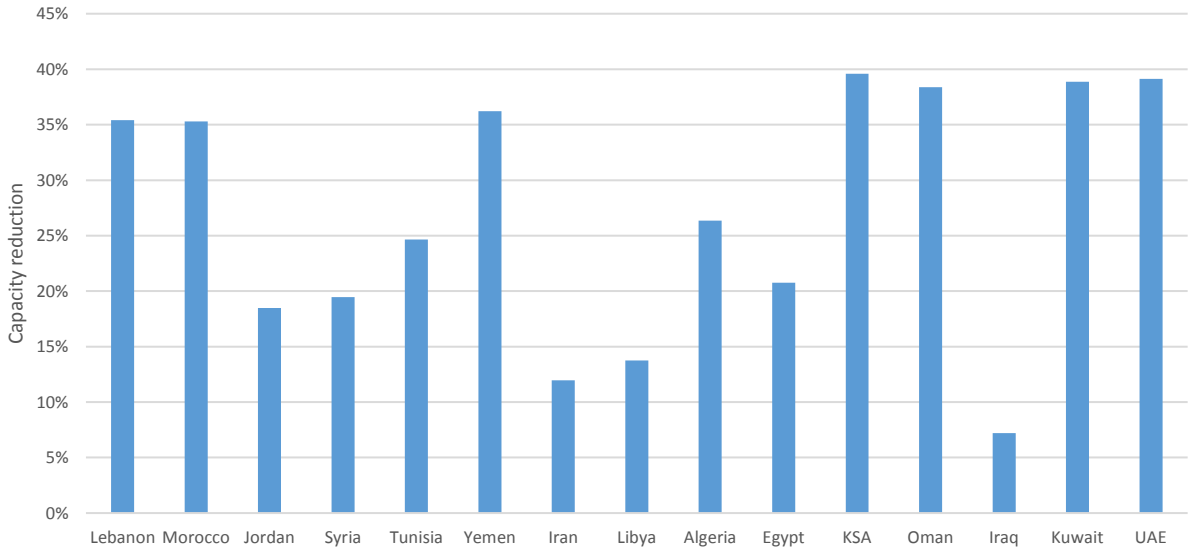

Figure 6-2 Reduction of required installed capacity between 2017 and 2030 scenarios

Figure 6-2 shows that the relative reduction of necessary installed capacity is very significant in some countries, beyond 35% in some of them, with a maximum for Saudi Arabia. The lowest

reduction is expected to happen in Iraq, where the reduction would be around just 7%. The justification for this disparity is explained by the different adequacy of the two analyzed technologies. Apparently, in those countries where there is not a very predominant technology (i.e. Iraq, as shown in Figure 6-3), the reduction is low because the system is better optimized by having a mix of both of them. However, for countries where there is a clear predominant technology (i.e. Saudi Arabia as shown in Figure 6-3), the reduction on installed capacity is much more significant because the optimized system becomes monopolized by that technology.

Analyzing the share between both technologies, Figure 6-3 depicts how each technology evolves in each country. While some countries have a parallel reduction of technologies (Iran, Iraq, etc.), other countries show a clear dominance of one technology over time and a drastic reduction on the other (Saudi Arabia, UAE, etc.).

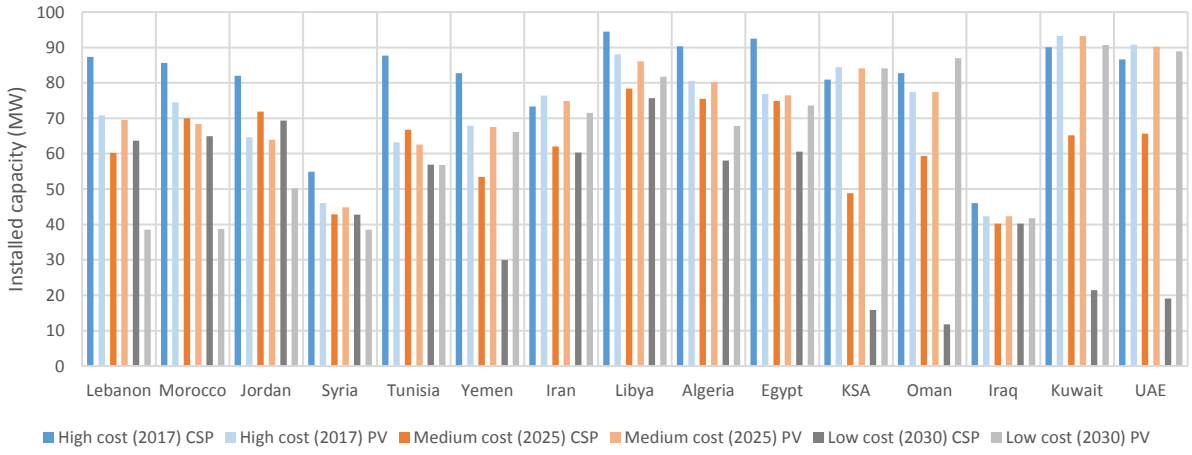

Figure 6-3 Installed capacity of CSP and PV in the three scenarios

However, this figure cannot be fully interpreted by just looking the evolution of each technologies. Its interpretation requires further analysis as detailed in the following sections.

6.2. Generation deployment

The analysis has been carried out considering just two absolute sources (CSP and PV), the analysis of generation pool is very simple. It can be reduced to the analysis of one of the two. Figure 6-4 shows the percentage of energy that is produced by CSP in each scenario.

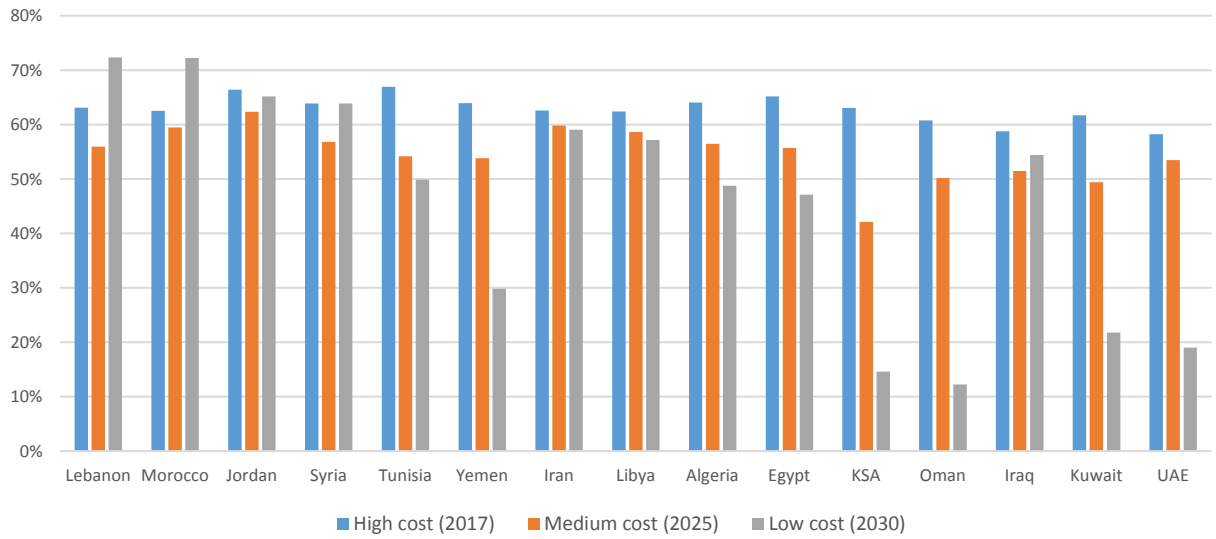

Figure 6-4 Percentage of energy produced by CSP in the three scenarios

In scenario with high prices (2017), the predominant technology for all the countries is CSP, with shares above 50%. Even in 2025, the CSP keeps being the major electricity source in most of the countries except Saudi Arabia and Kuwait. However, the drastic change occurs in the 2030 (low costs scenario), when in most of the countries the share is similar for both technologies. Still, there are some exceptions in both extremes. CSP keeps its predominance in countries such as Lebanon, Morocco, Jordan and Syria, while it is very minor in others: Saudi Arabia, Oman, Kuwait and UAE. The explanation for this repartition is fully explained by the ratio DNI/GHI depicted in Figure 5-7. Countries with the higher DNI/GHI ratio tends to keep CSP as main technology while the countries with lower ratios keep relying in PV.

Key conclusion

Considering the expected forecasts for the technologies cost evolution, cost will not be the only and/or main driver to decide whether CSP or PV is more suitable in a specific location. The availability of their respective solar resource will remain as a critical factor for optimizing the generation mix. The fact that each solar technology relies in one type of radiation (DNI or GHI) is a key element that need to be always considered.

6.3. Storage deployment

The expected evolution of storage cost, as it was shown in the previous section, will be the main driver that will change the configuration of solar power generation in the countries. Figure 6-5 depicts the amount of storage installed for each technology in the respective scenarios. In most of the countries, the thermal storage (TES) associated with CSP is higher than battery storage (BESS) associated with PV. Nevertheless, in countries such as Saudi Arabia, Oman, UAE or Iraq, the BESS is very similar or higher than TES in 2030. This is also explained by the ratio DNI/GHI depicted in Figure 5-7. Countries with the higher DNI/GHI ratio tend to keep CSP and TES as main technology while the countries with lower ratios keep relying in PV and BESS.

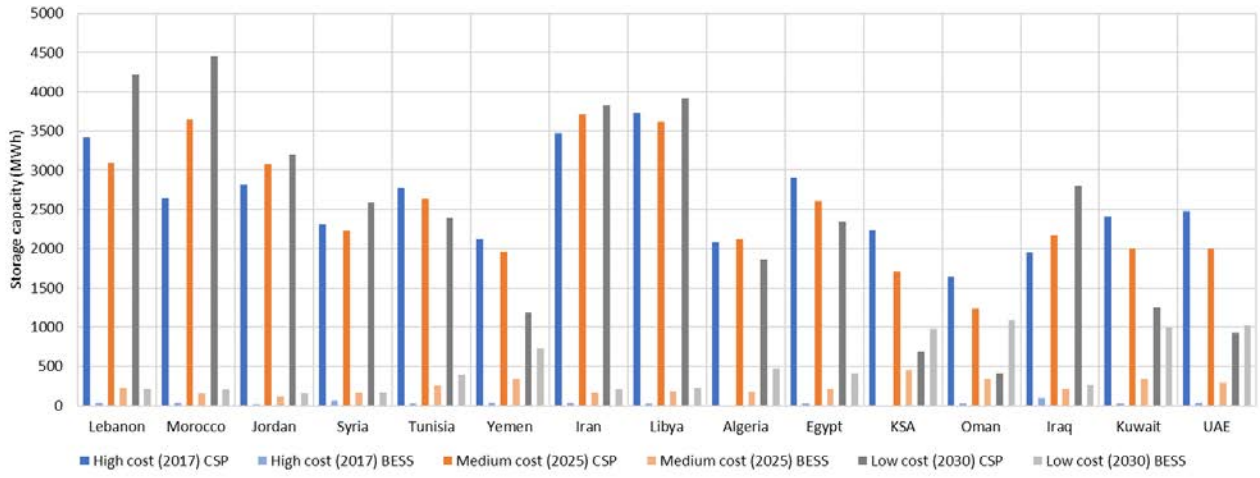

Figure 6-5 Installed storage capacity for CSP (TES) and PV (BESS) in each scenario

Key conclusion

Storage associated with CSP is heavily predominant over BESS. Even when the costs fall drastically down in 2030, thermal storage seems to be a more cost-efficient option for energy storage in most cases.

As the cost of battery storage is falling, the percentage of energy generated by the PV+BESS system is increasing, as so does the energy share from BESS, that is, the generation displaced to non-daylight time. Figure 6-6 shows the percentage of energy that is supplied to the grid by the BESS from the total generated by PV. To highlight that countries with the highest GHI progressively increase the percentage over time reaching more than 50% in 2030 in places as Saudi Arabia, Oman, Kuwait and UAE.

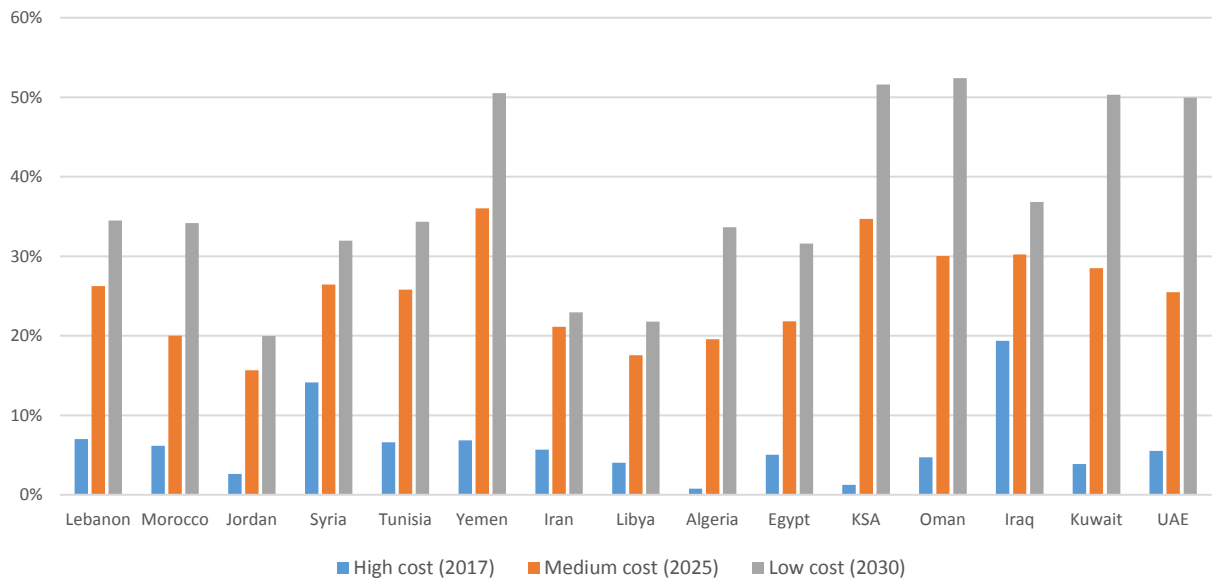

Figure 6-6 Percentage of energy generated by PV that is supply from BESS

6.4. Unserved energy

The unserved energy is defined as the amount of energy that is not covered by the generation from either CSP or PV. The results for the different scenarios (Figure 6-7) show that the unserved energy in all scenarios and countries is kept relatively low. Unserved energy is below 3% in the majority of countries in scenarios with higher cost (2017). In the low-cost scenario (2030), practically all countries have unserved energy between 1,5% and 0.5%. Just Kuwait is the exception keep an almost 2% of unserved energy in this 2030 scenario.

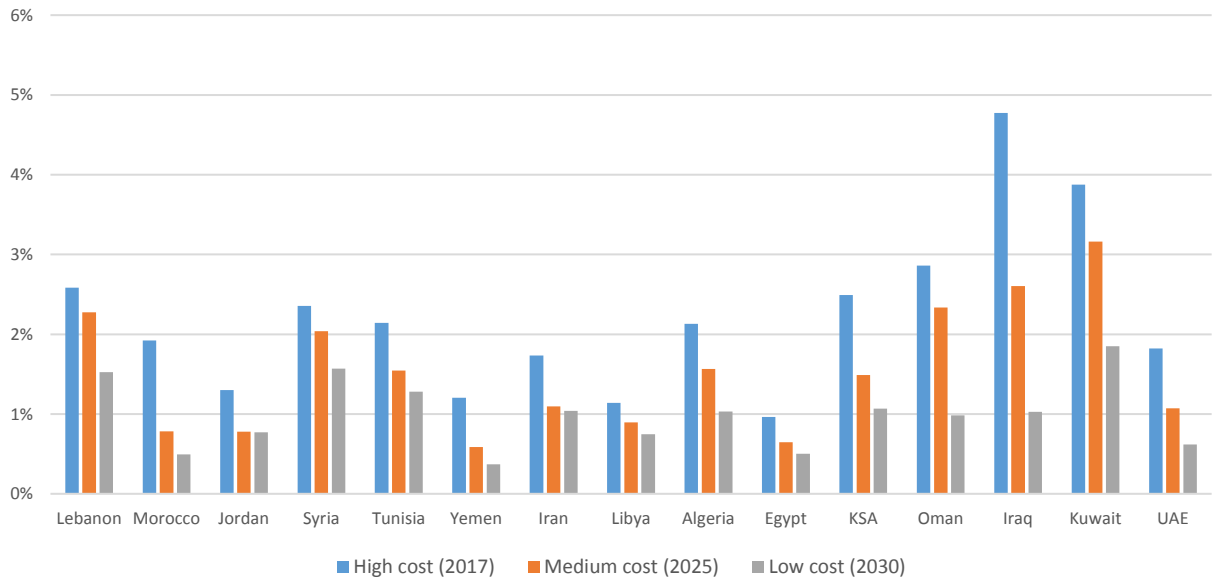

Figure 6-7 Unserved energy

6.5. Cost of energy

Based on the cost structure defined for each scenario, the model calculates the Levelized Cost of Energy in each case and country. Obviously, the electricity cost decreases as component costs are decreasing. Figure 6-8 shows the cost evolution.

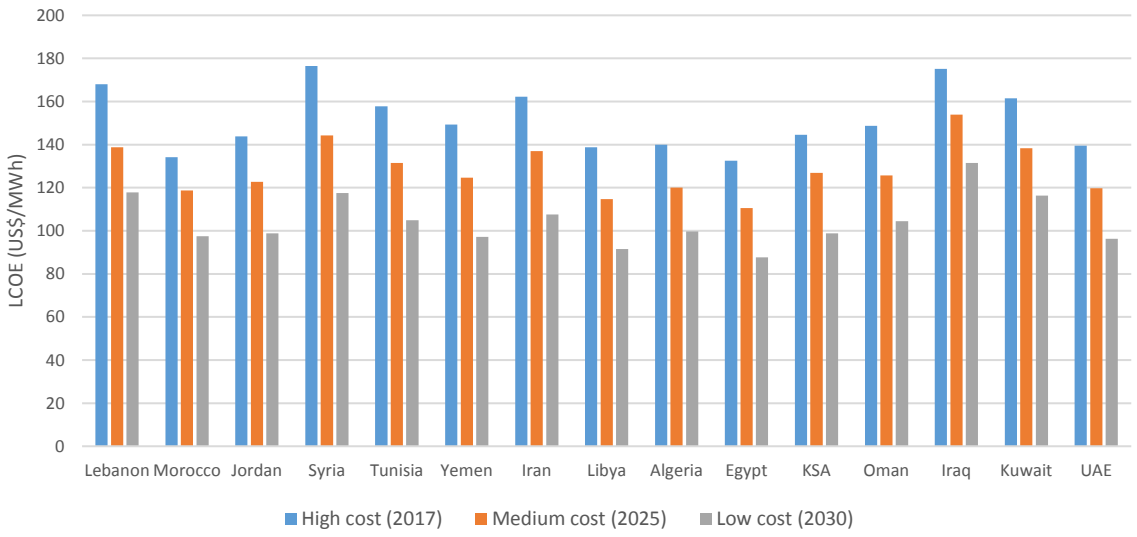

Figure 6-8 Evolution of LCOE

In the high cost scenario (2017) the base load with solar would have a cost between US$130/MWh and US$180/MWh. In the medium cost scenario (2025) the costs go between US$110/MWh and US$150/MWh. Finally, in the low-cost scenario (2030) the costs further drop to a range between US$90/MWh and US$120/MWh. Although in a global perspective these are high costs for generating baseload electricity as shown in Figure 6-9 (IEA 2015), one needs to consider that many of MENA countries still rely on oil based generation for baseload electricity, which implies much prices close to US$150/MWh.

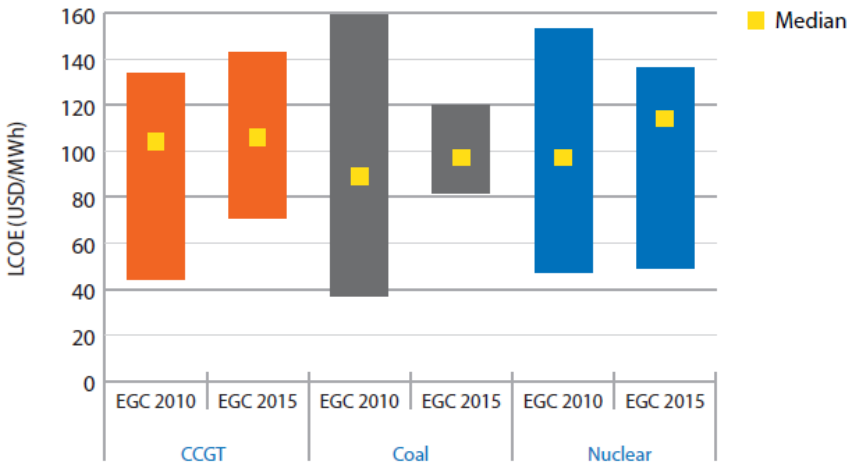

Figure 6-9 LCOE of baseload technologies (IEA, Projected Costs of Generating Electricity 2015)

Key conclusion

Solar-only systems are, in general terms, still far from being a competitive option when compared with conventional sources, although, if costs evolution is as expected, it might be in line with them by 2030. However, in countries where baseload is based on oil fired plants, solar baseload might be competitive. Moreover, this analysis does not include any carbon policies or carbon trade schemes that may happen in the future, which would change the perspective and conclusions of the analysis.

6.6. Correlations

Analyzing the different results and parameters from the model, the study tries to look for possible correlations among the different parameters and results. Those correlations would be very useful for explaining the different mechanisms involved in the decision-making process. It would also help to forecast system behaviors based on boundary conditions, namely, demand profiles and radiation levels.

6.6.1. Generated energy from CSP and PV

Figure 6-10 shows the relationship between the ratio of annual energy generated by CSP and annual energy generated by PV versus the ratio between country DNI and GHI. Each point represents the value for one country out of the analyzed fifteen countries. A linear regression has been included for each scenario to approximatively showing the evolution. The lines indicate that for higher prices (2017 and 2025, the predominance of one technology against the other is not dependent on radiation but very constant. However, in the scenario of lower price (2030) the regression indicates that there is a relationship between both ratios: higher the dominance of DNI higher the amount of CSP. In

this case, the radiation ratio is a more important factor than technology cost. This is due to the better behavior of thermal storage against batteries when costs are relatively low for both technologies.

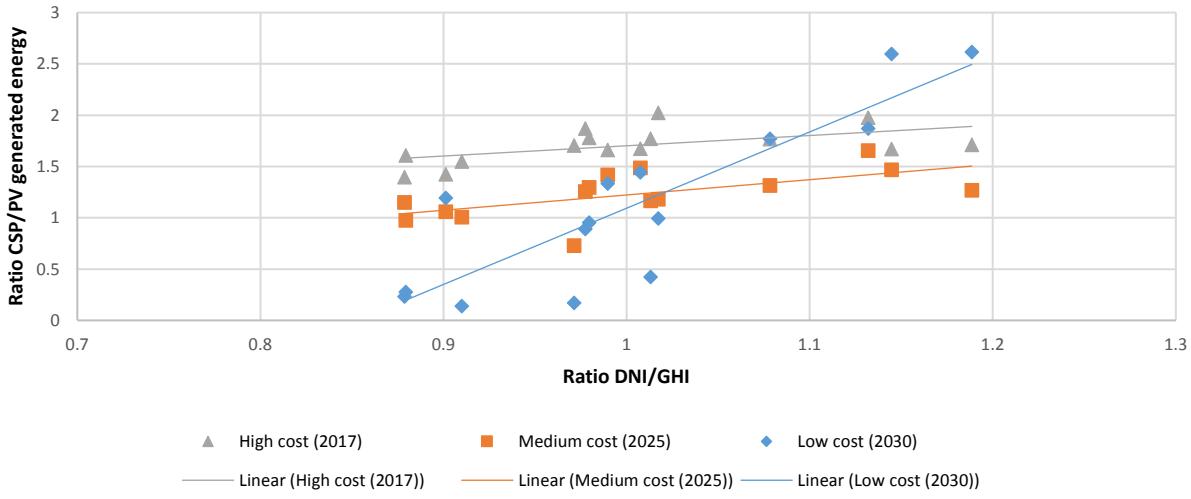

Figure 6-10 Ratio CSP/PV generation vs Ratio DNI/GHI

Key conclusion

Assuming the costs of each technologies evolve as currently expected, there might be a tipping point between 2025 and 2030, where the key factor to define the technology predominance (ratio CSP/PV) will be clearly determined by radiation while cost will play a secondary role.

6.6.2. LCOE

Figure 6-11 shows the relationship between the combined LCOE and the ratio between country DNI and GHI. Linear regressions have also been included for analyzing the trends in each scenario. Differing from the previous relationship, the LCOE does not show any link with the radiation in the country. Of course, LCOE levels are affected by technologies cost but the different shares in scenarios do not affect the combined electricity price. This is understandable considering that the

model always optimizes the cost of the electricity, modifying the mix of technologies to reach the minimum cost in every country and scenario.

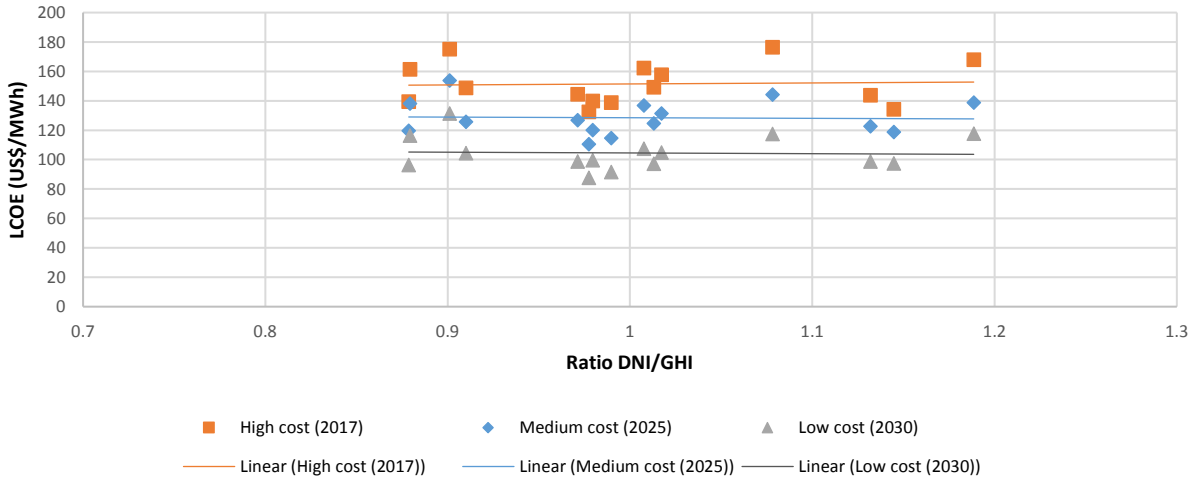

Figure 6-11 LCOE generation vs Ratio DNI/GHI

7. Analysis in specific countries: Jordan and UAE

After the analysis was carried out for the fifteen countries, it is clear that the diversity in behaviors across the region is very significant. Therefore, it would be interesting to analyze one example in each one of the two extremes of those behaviors (low DNI versus high DNI). For this study, and following the results obtained previously, Jordan and UAE seem very appropriate to have a clear understanding of the different performances of solar power in the region.

Jordan has a very good direct radiation (DNI) allowing a good performance of CSP and not a bad global radiation (GHI) suitable for PV. On the contrary, the UAE has a bad DNI but good GHI. For these two countries, the study will focus on two aspects: the daily generation in each of the time scenarios (2017, 2025 and 2030) and the sensitivity of solar technology selection based on different

financial conditions for the projects. For that purpose, the model has been run with three different WACC: 4%, 8%, 12%.

7.1. Daily profiles expected in Jordan and UAE

The daily profiles have been represented for specific singular periods of three days: during the summer solstice (20, 21 and 22 of June) and during the winter solstice (20, 21 and 22 of December). As it is shown in the sections below the differences are sensitive to the time scenario (technologies costs) and to the time of year (radiation).

Figure 7-1 and Figure 7-2 depict the different generation profiles for both countries and the three scenarios in summer and winter solstice respectively. As it is shown in the figure, the behaviors are diverging between countries over time. While in the 2017 scenario the profiles are quite similar, with mostly direct PV during daylight, CSP during non-daylight time and a small support of BESS, in 2030 the landscape changes completely. The solar deployment in both countries would be completely different and UAE will mostly rely on PV as baseload, with a very significant amount of BESS to supply the non-daylight time. Jordan, though, continues relying on CSP in 2030 scenario with a limited amount of direct PV for daylight and BESS for punctual support.

In winter solstice the use of battery storage (BESS) is more predominant during non-daylight time. Even in Jordan, where deployment of BESS is reduced, the support of BESS is essential at some hours when the system is almost entirely supplied by BESS.

7.2. Variation of technologies deployment with WACC

For Jordan and the UAE, the model has been run for different financial conditions (WACC). As is well known, project amortizations are very dependent on equity and debt interest combination, whatever is the share of each of them. Having in mind that solar projects do not have important

operational cost linked to the generation and, in particular, to fuel costs, the amortization is fully linked to the financial condition of the capital expenditure necessary to build the plant. In this regard, the cost of the energy generated by each technology is strongly dependent on financial conditions and the share between equity and debt (WACC).

All modeling described in this study until now has been performed considering a base-case financial conditions of WACC=8%, as indicated in section 5.4. However, conclusions may differ considerably under different financial conditions. In order to assess the extent to which different WACC values affect the optimal share of CSP and PV, his study has additionally applied two different conditions: a lower WACC (4%) and a higher WACC (12%).

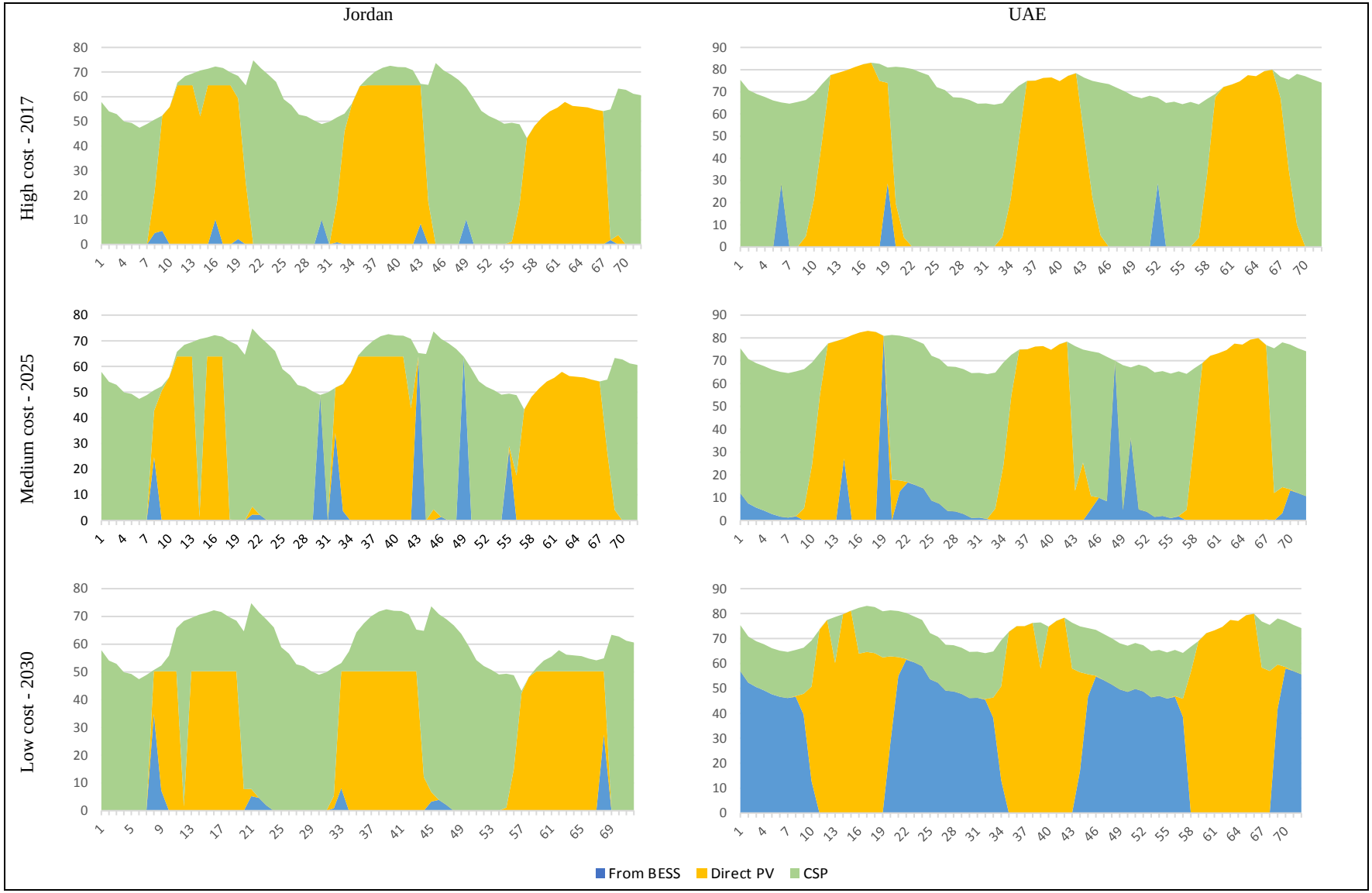

Figure 7-1 Daily generation profiles in summer solstice in Jordan and UAE

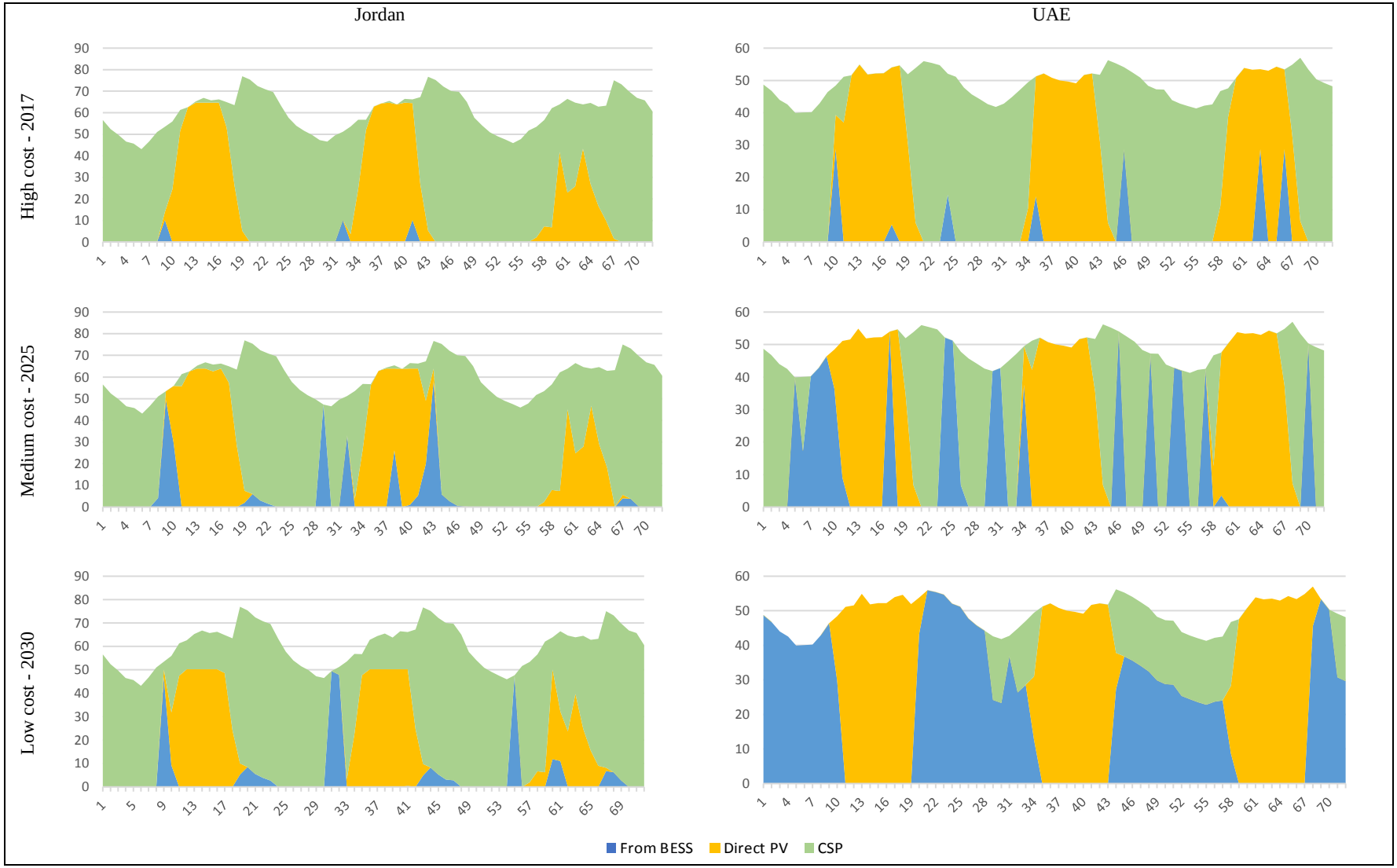

Figure 7-2 Daily generation profiles in winter solstice in Jordan and UAE

7.2.1. Sensitivity of required installed capacity with WACC

The installed capacity required to satisfy the demand (Figure 7-3) remains very similar in both countries with the change of WACC. Still, as it could have been foreseen, more expensive financial resources (higher WACC) implies less installed capacity and more unserved energy. The system, hence, is optimized by leaving some demand unserved because the cost of installing additional resources (solar capacity) is higher.

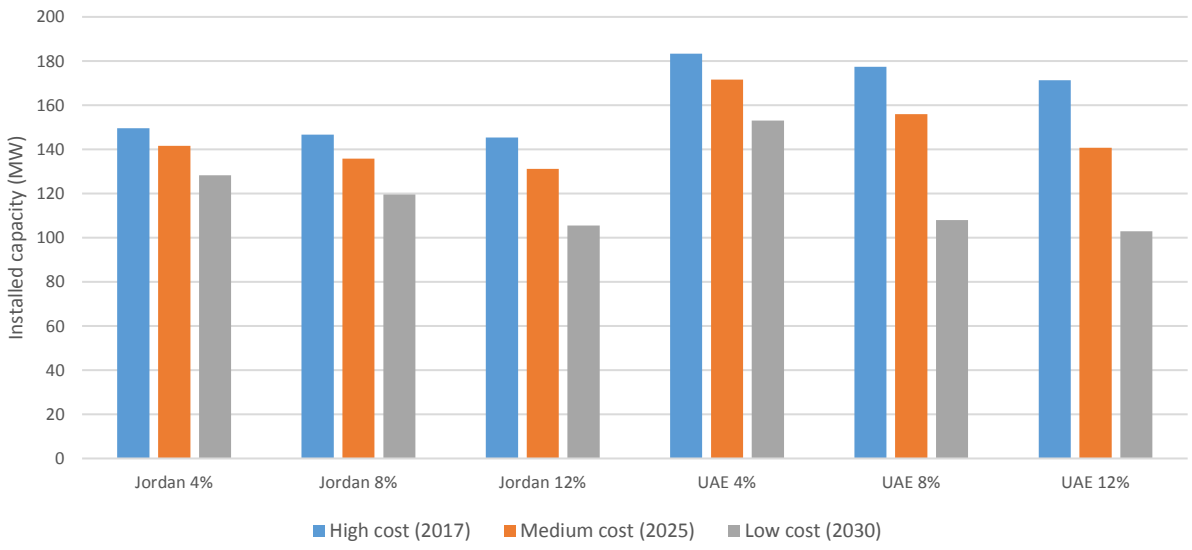

Figure 7-3 Total installed capacity in each scenario and WACC

In terms of the capacity installed of each technology, the higher the WACC is, the higher the tendency towards PV. In Jordan, although always the CSP is predominant, the increase in WACC reduces the difference between installed CSP and PV. In UAE, being PV the predominant, the gap between PV and CSP increases as WACC does. This is explained by the higher CAPEX required to install CSP per MW. The concentrating technology, CSP, is more capital intensive, so it is more affected by increases in cost of financial resources.

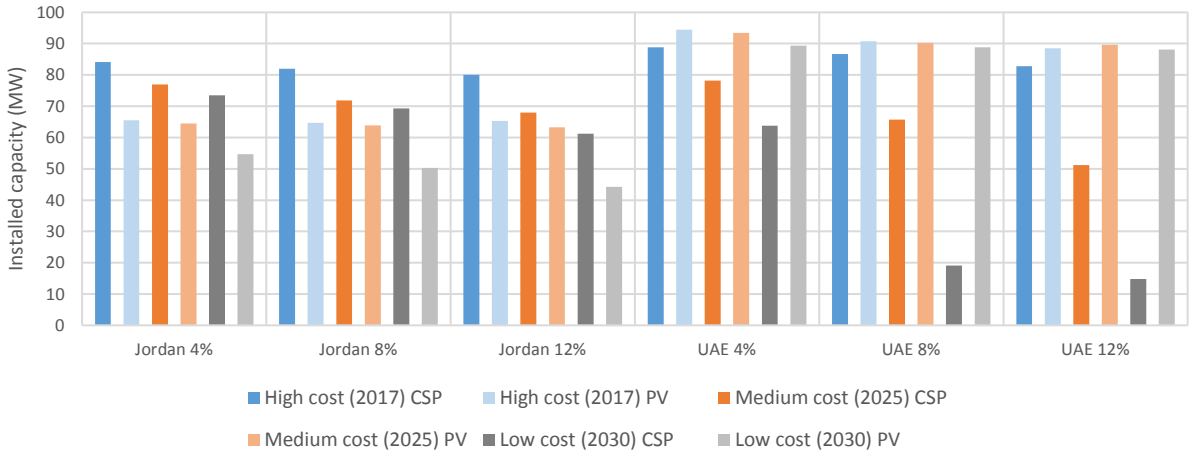

Figure 7-4 Total installed capacity of CSP and PV in each scenario and WACC

7.2.2. Sensitivity of energy generation with WACC

The variation of four parameters with WACC are analyzed in this section: percentage of energy from CSP, installed storage capacity, percentage of PV energy supply from the BESS and unserved energy.

The percentage of energy supply by CSP remains very similar across the different WACC cases in Jordan (Figure 7-5). However, in the UAE, with less predominance of CSP resources, the percentage is significantly reduced, mainly in the Medium cost (2025) scenario. In that scenario an increase from 8% to 12% reduces the amount of CSP in more than 10%. The low preference for CSP in UAE is, somehow, accentuated by the higher cost of the capital, discouraging even more the generation from CSP.

Regarding the installed capacity of storage, Figure 7-6 depicts the optimum amount of storage to be installed in each scenario. In Jordan, the increase of WACC implies a slight reduction on TES storage and a slight increase in BESS capacity. Again, the much better resources for CSP in this country favors the installation of this technology even with higher financial costs. In the UAE, though, the impact of financial cost is significant. With lower WACC, the amount of TES is very

much favored against BESS, but the increase of financial costs drastically changes the preferences for BESS.

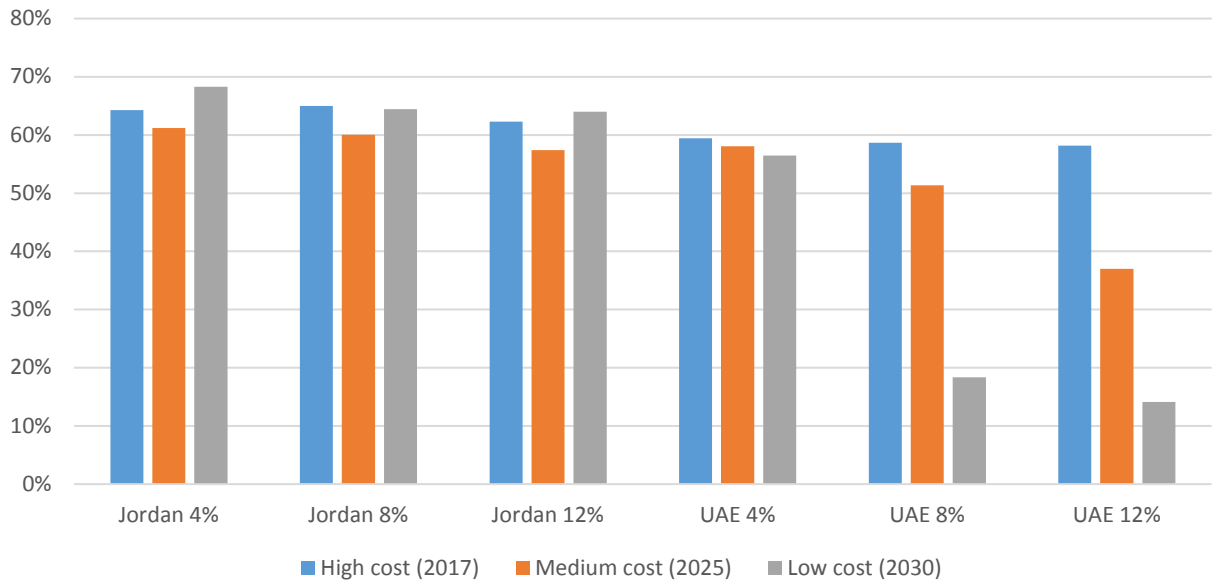

Figure 7-5 Percentage of annual energy supplied by CSP in each scenario and WACC

The conclusions above are also supported by the results shown in Figure 7-7, depicting the percentage of energy from PV that is supplied from the BESS. While in Jordan this percentage remains very constant throughout the different WACC values, in the UAE the percentage increases drastically in cases of medium cost (2025) and low cost (2030). In those cases, the percentage of energy from BESS triples and quintuples, respectively.

Furthermore, the unserved energy increases with the financial cost (Figure 7-8). Obviously, if the financial resources are more expensive, the systems tend to leave some energy unserved instead of installing additional capacity. Again, the UAE is more sensitive to changes in WACC values, particularly in the high cost scenario (2017), where CSP is relatively more favored than in the lower cost cases given its high technology cost. However, as costs are dropping in the subsequent scenarios, the energy share shifts towards PV+BESS and the unserved energy is reducing. One

important conclusion is that in the low-cost scenario (2030) the higher costs of capital tends to equal the unserved energy in both countries. While at 4% Jordan has more unserved energy, at 12% the values are very similar. Once more, this is due to the higher predominance of CSP in Jordan and the higher dependence of CSP on financial costs.

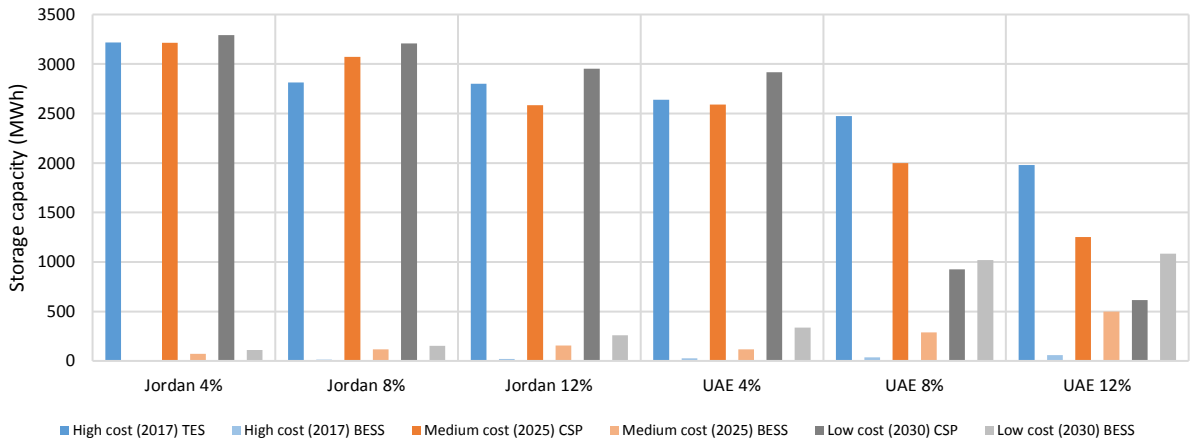

Figure 7-6 Installed storage capacity installed for CSP (TES) and PV (BESS) in each scenario and WACC

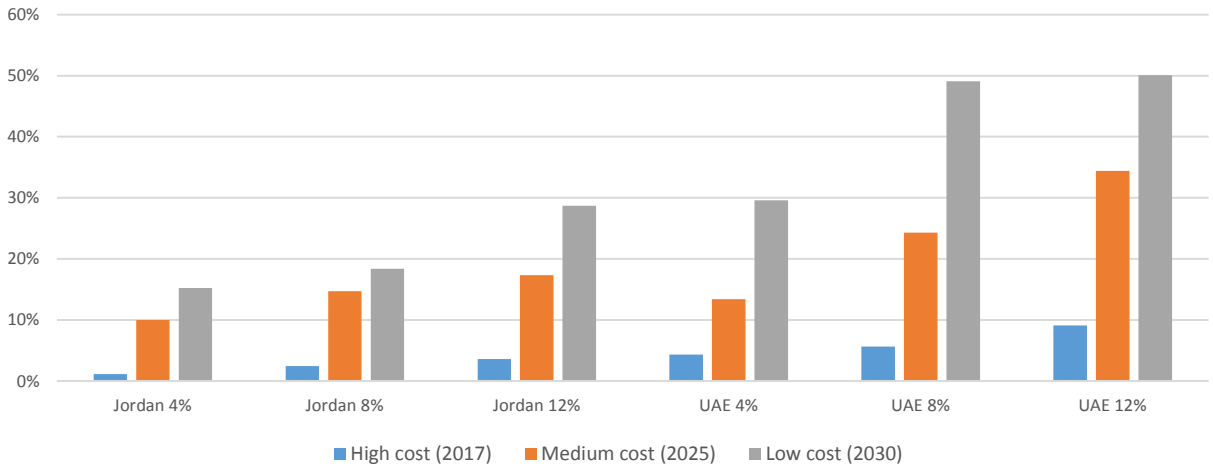

Figure 7-7 Percentage of energy generated by PV that is supply from BESS in each scenario and WACC

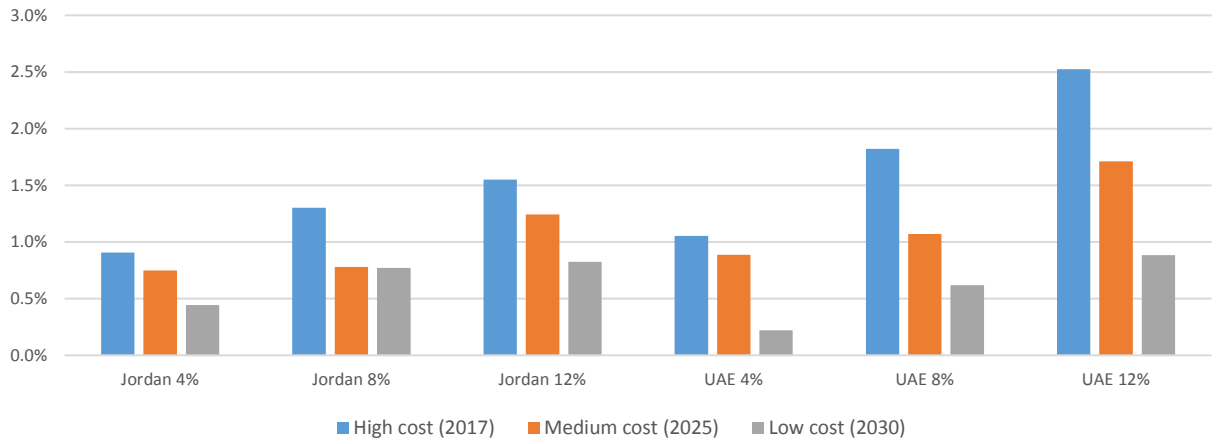

Figure 7-8 Unserved energy in each scenario and WACC

Key conclusion

The increase in financial costs favors the installation of PV+BESS instead of CSP. Being CSP a more capital-intensive technology (higher cost per installed MW), the WACC has an important role to play in the definition of optimum generation mix.

7.2.3. Sensitivity of LCOE with WACC

Figure 7-9 shows the evolution of LCOE in each scenario with the different WACC values tested. As it could be expected, the cost of electricity increases significantly with the cost of capital. However, the Jordan system is more sensitive to financial cost increases than the UAE one. The explanation is the predominance of CSP versus PV. Jordan solar resource for PV is not as good as for CSP, therefore, the increase of financial costs does not change the predominance of CSP but increases the average price of electricity. In UAE, the increase of financial cost is somehow compensated by the higher amount of PV due to the existing good resource for this technology. Being PV less affected by financial costs, the cost of electricity, although higher, is still lower than that in Jordan.

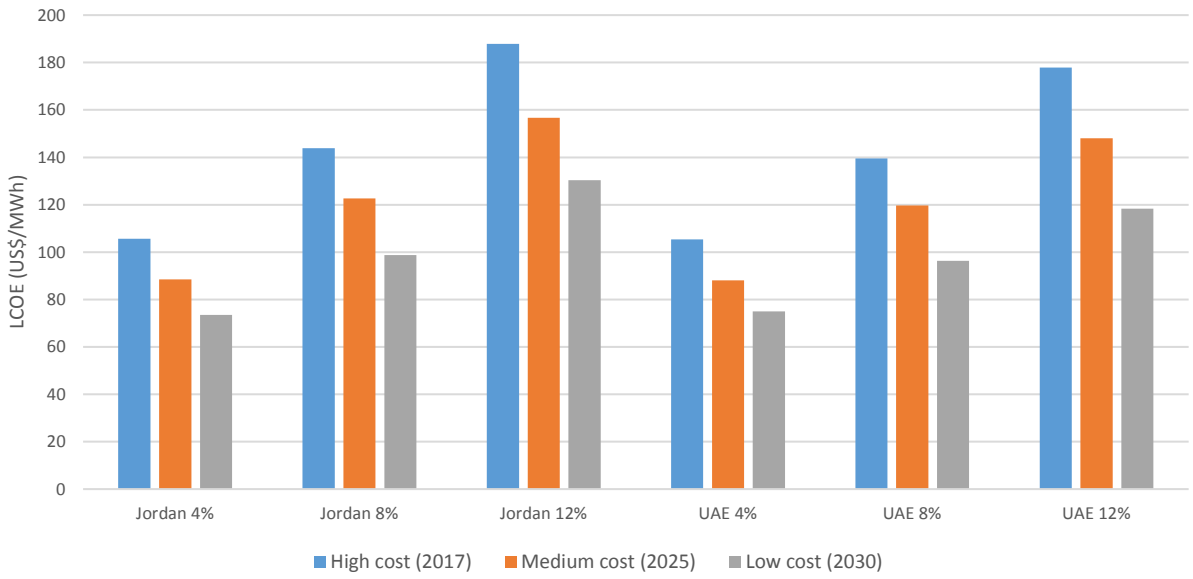

Figure 7-9 Sensitivity of LCOE with each scenario and WACC

8. Conclusions

This study intends to shed some light about how two solar technologies—namely solar photovoltaics with battery systems and concentrated solar power—can coexist in a power system and how we can compare the techno-economic performance of both on a level playing field

The study focuses on fifteen countries in the Middle East and North African region (MENA), where the study assumes that demand can only be supplied by solar power. Two technologies are analyzed: Concentrating Solar Power (CSP) with Thermal Energy Storage (TES) and Photovoltaics (PV) with Battery Energy Storage System (BESS).

For the solar resource values in different countries, DNI and GHI have been modeled in specific points of the countries, where the radiations are average, avoiding locations with extreme radiation (higher or lower).

The analysis is based on a linear programming model that minimizes the annual cost of electricity generation following the load profile and radiation in each country. A common base of 100 MW peak demand has been adopted for the sake of simplicity and comparability.

As it was set in the introduction, the objective of this study is to respond to two key questions related to the future of renewable solar energy and its role in future power systems. The response to those questions are the base of these conclusions.

Question #1: Can solar technologies only supply an entire national and/or regional power systems from a demand point of view at an affordable cost?

The study shows solar only (with storage) can be a feasible alternative for providing power to an entire system. The unserved energy in each case would be low and the flexibility is guaranteed by the storage capacity in both technologies.

On the economic side, solar technologies are still far from being a competitive option when compared with conventional sources, although, if costs evolution is as expected, it might be in line with them by 2030. However, in countries where baseload is based on oil fired plants solar baseload might be already competitive. This analysis does not include the difficult-to-measure benefits associated with a power system based on clean energy, nor the economic and financial effects of a possible carbon policy or carbon trade scheme, which may happen in the future, and change the analysis perspective and conclusions.

Question #2: Considering the expected improvements in technologies and prices of the different solar technologies and storage systems, what technology can be expected to have the most promising future to entirely supply the whole demand of a power system at a competitive cost? In other words, what are the drivers that define the adequacy of a solar technology in a specific geographical location?

The study shows that, assuming the expected forecasts for the technologies cost evolution, cost will not be the only and/or main driver. The availability of their respective solar resource will continue to be a critical factor for optimizing the generation mix. The fact that each solar technology relies in one type of radiation (DNI or GHI) is a key element that need to be always considered. The reduction in technologies costs that are expected in the forthcoming years, instead of defining a global predominant solar technology, will only accentuate the dependency on the respective solar resource. Moreover, this adequacy of solar resource for each technology will become the main criteria to determine an optimum deployment of solar generation in specific locations as technologies costs decrease. Assuming the costs of each technologies evolve as currently expected, there might be a tipping point between 2025 and 2030, where the key factor to define the technology predominance (ratio CSP/PV) will be clearly determined by radiation while cost will play a secondary role.

The study also shows that solar technologies are complementary in almost all scenarios. Whatever is the cost evolution both technologies are always present and none of them is completely discarded.

In terms of storage technologies, the study shows that thermal storage associated with CSP is heavily predominant over BESS. Even when the costs are expected to fall drastically down in the coming 10-15 years, the thermal storage seems a better cost-benefit option for energy storage in most cases. Again, the selection would be, hence, based in the primary source of energy, whether this is thermal (CSP) or electric (PV) rather than in the storage technologies themselves.

9. Bibliography

Breeze, Paul. 2014. *Power Generation Technologies.* Elsevier.

Creara. 2017. *Application Note Medium Size PV plants.* European Copper Institute.

Ehrhart, B. and Gill, D. 2014. "Evaluation of annual efficiencies of high temperature central receiver concentrated solar power plants with thermal energy storage." *Energy Procedia* 752-761.

EIA. 2017. *Levelized Cost and Levelized Avoided Cost of New Generation Resources in the Annual Energy Outlook 2017.* Energy Information Agency.

EU. 2016. *Identification of Appropriate Generation and System Adequacy Standards for the Internal Electricity Market.* European Commission.

Falcone, P.K. 1986. *A handbook for solar central receiver design* . SANDIA.

Feldman D., Margolis R., and Denholm P. 2016. *Exploring the Potential Competitiveness of Utility-Scale Photovoltaics plus Batteries with Concentrating Solar Power, 2015–2030.* NREL.

IEA. 2010. *Projected Costs of Generating Electricity.* International Energy Agency.

IEA. 2015. *Projected Costs of Generating Electricity.* International Energy Agency.

IEA. 2016. *World Energy Outlook.* International Energy Agency (IEA).

IRENA. 2012. *Concentrating Solar Power.* IRENA.

IRENA. 2017. *REthinking Energy 2017.* IRENA.

J. Jorgenson, P. Denholm, and M. Mehos. 2014. *Estimating the Value of Utility-Scale Solar Technologies in California Under a 40% Renewable Portfolio Standard.* NREL.

Kalogirou, Soteris A. 2013. *Solar Energy Engineering.* Academic Press.

Kolb, Gregory. 2011. *An Evaluation of Possible Next-Generation High-Temperature Molten-Salt Power Towers.* SANDIA.

Lazard. 2016. "Lazard's Levelized Cost of Energy Analysis."

Lazard. 2016. "Lazard's Levelized Cost of Storage Analysis."

M.J. Montes, A. Abánades , J.M. Martínez-Val , M. Valdés. 2009. "Solar múltiple optimization for a solar-only thermal power plant, using oil as heat transfer fluid in the parabolic trough collectors." *ETSI.*

Manuel Romero-Alvarez, Eduardo Zarza. 2007. "Concentrated Solar Thermal Power." In *Handbook of Energy Efficiency and Renewable Energy*, by Frank Kreith D. Yogi Goswami, 21-1, 21-92. Boca Raton, FL: CRC Press.

Manuel Silva, PhD. 2005. *Sistemas termosolares de concentración.* University of Seville.

NERC. 2016. *Probabilistic Assessment.* North America Electric Reliability Corporation.

NREL. 2007. "System Advisory Model (SAM)."

NREL. 2013. *Weather-Corrected Performance Ratio.* NREL.

Patsiosa, Charalampos. 2016. "An integrated approach for the analysis and control of grid connected energy storage systems." *Journal of Energy Storage* (Journal of Energy Storage) 48-61.

Quaschning, Volker. 2004. "Photovoltaic systems. Technology Fundamentalrs." *Renewable Energy World* 81-84.

Solar Radiation Monitoring Laboratory. University of Oregon. 2002. http://solardat.uoregon.edu/SolarRadiationBasics.html.

The Economist. 2011. "Securing MENA’s electric power supplies to 2020."

Vignola, Frank, Fotis Mavromatakis, and Jim Krumsick. 2008. "Performance of inverters."

APPENDIX 1. Linear programming model

Scalars

NominalPlantPeak Peak generation /100/

PerformanceCSP_Receiver Efficiency receiver)- Efficiency solar field is included in data /0.86/

CSP_Auxiliaries Porcentage auxiliaries /0.035/

CSPTurbEfficiency Efficiency power cycle CSP /0.41/

DesignPointReceiver Radiation for design point in receiver kW per m2 /1/

CSPStorage_Eff Efficiency CSP storage round trip /0.98/

PV_panel_Efficiency Efficiency of PV panels /0.18/

Performance_Ratio Efficiency PV without Inverter /0.91/

InverterEfficiency /0.93/

PV_Auxiliaries Porcentage auxiliaries /0.02/

PVStorage_Eff Efficiency batteries including auxiliaries /0.88/

PVSTY_N PV storage yes 1 or not 0 /0/

CostUnserved cost of energy non served /1000/

EnergyPrice incomes per MWh /200/

;

Sets

t hours of day /1*8760/

d day type /Workday/

r regions /Jordan, Egypt, KSA, UAE, Oman, Kuwait, Iraq, Yemen, Libya, Tunisia, Morocco, Algeria, Lebanon, Syria, Iran/

a cost areas /SFCSP, RECSP, STCSP, PBCSP, SFPV, STPV, PBPV/

;

Parameter LocationIndex(r) Location Index

/

Jordan 1 Egypt 2 KSA 3 UAE 4 Oman 5 Kuwait 6 Iraq 7 Yemen 8 Libya 9 Tunisia 10 Morocco 11 Algeria 12 Lebanon 13 Syria 14 Iran 15

/;

Variables

*Dimension variables

CSPArea(r) Area SF CSP (m2)

CSPNominalReceiver(r) Thermal design receiver (MWth)

CSPNomPower(r) Nominal gross power turbine CSP (MW)

CSPStorageCap(r) Storage capacity CSP (MWh th)

CSPEnergy(r) CSP annual energy (MWh)

CSPfromStorage(r) Total energy from storage

DNI(r) Radiation for CSP (kWh per m2 y)

PVArea(r) Area SF PV (m2)

PVNomPower(r) Nominal power turbine PV (MW)

PVStorageCap(r) Storage capacity PV (MWh)

PVEnergy(r) PV annual energy (MWh)

PVfromStorage(r) Total energy from storage

GHI(r) Radiation for CSP (kWh per m2 y)

Unserved(r)

* Generation/operation variables

CSPThermalField(r,t) Thermal energy generated by CSP solar field (MWh th)

*CSPThermalSG(r,t) Thermal energy generated by CSP direct to generation (MWth)

CSPThermalStorageIn(r,t) Injection to CSP storage (MWh th)

CSPThermalStorageOut(r,t) Withdrawal from CSP storage (MWth)

CSPThermalStorageLevel(r,t) Level of CSP storage (MWth)

CSPThermalReceiver (r,t) thermal power to the receiver

CSPGenPower(r,t) Generation from CSP (MW)

PV_DCSolarField(r,t) Generation DC energy by PV solar field (MWh)

PV_DCDirect(r,t) Electric energy generated by PV direct to generation (MWh)

PV_DCStorageIn(r,t) Injection to PV storage (MWh)

PV_DCStorageOut(r,t) Withdrawal from PV storage (MWh)

PV_DCStorageLevel(r,t) Level of PV storage (MWh)

PVGenPower(r,t) Generation from PV (MW)

Incomes (r) Incomes due to price

* Violation variables

USE(r,t) Unserved demand (MW)

Cost

;

Positive variables CSPArea, CSPNominalReceiver, CSPThermalReceiver, CSPNomPower, CSPStorageCap, CSPEnergy, CSPThermalField, CSPThermalSG, CSPThermalStorageIn, CSPThermalStorageOut, CSPThermalStorageLevel, CSPGenPower;

Positive variables PVArea, PVNomPower, PVStorageCap, PVEnergy, PV_DCSolarField, PV_DCDirect, PV_DCStorageIn, PV_DCStorageOut, PV_DCStorageLevel, PVGenPower, USE, USE_RES;

Equations

*CSP equations

CSPSolarFieldGeneration(r,t) Generation in CSP solar field

CSPReceiver (r,t) Thermal balance in the receiver

CSPReceiver1 (r,t) Thermal balance in the receiver

CSPReceiver2 (r,t) Thermal balance in the receiver

CSPStorBal(r,t) Storage balance for hour > 1

CSPStorBal1(r,t) Storage balance for hour 1

CSPDirectGeneration(r,t) Direct generation from CSP

CSPGeneration(r,t) Generation CSP

CSPMinLoad(r,t) Minimum Load CSP turbine

CSPCap(r,t) Capacity CSP

CSPTotalEnergy(r)

TotalDNI(r)

*PV equations

PVSolarFieldGeneration(r,t) Generation in PV solar field

PVStorBal(r,t) Storage balance for hour > 1

PVStorBal1(r,t) Storage balance for hour 1

PVDirectGeneration(r,t) Direct generation from CSP

TotalGHI(r)

PVGeneration(r,t)

PVCap(r,t) Generation PV

PVTotalEnergy(r)

CSPEnergyStorage(r) Energy from Storage in CSP

PVEnergyStorage(r) Energy from Storage in PV

OnewayStorage1(r,t) Storage can only run in one direction

*Revenues(r)

UnservedDemand(r) Unserved demand

DemBal(r,t) Demand-suply balance for energy

Obj Objective function - total system cost

CSPStorageLimit(r,t) Storage capacity limit

PVStorageLimit(r,t) Storage capacity limit

;

*equations CSP

CSPSolarFieldGeneration(r,t).. CSPThermalField(r,t)=l= (CSPProfile(t,r)*CSPArea(r))/1000000;

CSPReceiver(r,t).. CSPThermalReceiver(r,t)=e=CSPThermalField(r,t);

CSPReceiver1(r,t).. CSPThermalReceiver(r,t)=l=DesignPointReceiver*0.6*CSPArea(r)/1000;

CSPReceiver2(r,t).. CSPThermalReceiver(r,t)=l=CSPNominalReceiver(r);

CSPDirectGeneration(r,t)..
CSPThermalReceiver(r,t)*PerformanceCSP_Receiver=e=CSPThermalStorageIn(r,t);

CSPStorBal(r,t)$(ord(t)>1).. CSPThermalStorageLevel(r,t) =e= CSPThermalStorageIn(r,t)-CSPThermalStorageOut(r,t)+CSPThermalStorageLevel(r,t-1);

CSPStorBal1(r,t)$(ord(t)=1).. CSPThermalStorageLevel(r,t) =e= CSPThermalStorageIn(r,t)-CSPThermalStorageOut(r,t);

CSPThermalStorageLevel.fx(r,"1")=0;

CSPGeneration(r,t)..
CSPGenPower(r,t)=e=CSPStorage_Eff*CSPThermalStorageOut(r,t)*CSPTurbEfficiency*(1-CSP_Auxiliaries);

```
CSPMinLoad(r,t).. CSPGenPower(r,t)=g=CSPNomPower(r)*0;

CSPCap(r,t).. CSPGenPower(r,t)=l=CSPNomPower(r)*(1-CSP_Auxiliaries);

CSPStorageLimit(r,t).. CSPThermalStorageLevel(r,t)=l=CSPStorageCap(r);

TotalDNI(r).. DNI(r)=e=sum(t,CSPProfile(t,r));


*equations PV

PVSolarFieldGeneration(r,t).. PV_DCSolarField(r,t)=l=
(PVProfile(t,r)*PVArea(r)*PV_panel_Efficiency*Performance_Ratio)/1000000;

PVDirectGeneration(r,t).. PV_DCSolarField(r,t)=e=PV_DCDirect(r,t)+PV_DCStorageIn(r,t);

*PV_NoStorage(r,t).. PV_DCStorageIn(r,t)=e=0;

PVStorBal(r,t)$(ord(t)>1).. PV_DCStorageLevel(r,t) =e= PVStorage_Eff*PV_DCStorageIn(r,t)-
PV_DCStorageOut(r,t)+PV_DCStorageLevel(r,t-1);

PVStorBal1(r,t)$(ord(t)=1).. PV_DCStorageLevel(r,t) =e= PVStorage_Eff*PV_DCStorageIn(r,t)-
PV_DCStorageOut(r,t);

PV_DCStorageLevel.fx(r,"1")=0;

OnewayStorage1(r,t).. PV_DCStorageLevel(r,t) =g= PVStorage_Eff*PV_DCStorageIn(r,t);

PVGeneration(r,t)..
PVGenPower(r,t)=e=(PV_DCDirect(r,t)+PVStorage_Eff*PV_DCStorageOut(r,t))*InverterEfficie
ncy*(1-PV_Auxiliaries);

PVCap(r,t).. PVGenPower(r,t)=l=PVNomPower(r);

PVStorageLimit(r,t).. PV_DCStorageLevel(r,t)=l=PVStorageCap(r);

TotalGHI(r).. GHI(r)=e=sum(t,PVProfile(t,r));


*Global equations

CSPTotalEnergy(r).. CSPEnergy(r) =e= sum(t,CSPGenPower(r,t));

PVTotalEnergy(r).. PVEnergy(r) =e= sum(t,PVGenPower(r,t));

CSPEnergyStorage(r)..
CSPfromStorage(r)=e=sum(t,CSPStorage_Eff*CSPThermalStorageOut(r,t)*CSPTurbEfficiency*
(1-CSP_Auxiliaries));

PVEnergyStorage(r)..
PVfromStorage(r)=e=sum(t,PVStorage_Eff*PV_DCStorageOut(r,t)*InverterEfficiency*(1-
PV_Auxiliaries));

UnservedDemand(r).. Unserved(r)=e=sum(t,USE(r,t));
```

DemBal(r,t).. CSPGenPower(r,t)+PVGenPower(r,t)+USE(r,t)=e= Load(t,r)*ZoneShare(t,r)*NominalPlantPeak;

Obj.. Cost =e= Sum(r,((CSPArea(r)*SolarCost("SFCSP","Capex")+PVArea(r)*SolarCost("SFPV","Capex")+CSPNominalReceiver(r)*SolarCost("RECSP","Capex")+CSPStorageCap(r)*SolarCost("STCSP","Capex")

+CSPNomPower(r)*SolarCost("PBCSP","Capex")+PVNomPower(r)*SolarCost("PBPV","Capex"))*CRF25(r,"CRF")+PVStorageCap(r)*SolarCost("STPV","Capex")*CRF10(r,"CRF")+(CSPArea(r)*SolarCost("SFCSP","FixedOM")+PVArea(r)*SolarCost("SFPV","FixedOM")+CSPNominalReceiver(r)*SolarCost("RECSP","FixedOM")+CSPStorageCap(r)*SolarCost("STCSP","FixedOM")+PVStorageCap(r)*SolarCost("STPV","FixedOM")

+CSPNomPower(r)*SolarCost("PBCSP","FixedOM")+PVNomPower(r)*SolarCost("PBPV","FixedOM")) + sum(t,USE(r,t)*CostUnserved)))

Solving

Model CSP /all/;

Solve CSP using LP min cost;